College of Saint Benedict and Saint John's University

DigitalCommons@CSB/SJU

2013

Differential Modeling and Efficiency Testing of the Saint John's University Cogeneration Power Plant

Richard J. Kirchner
College of Saint Benedict/Saint John's University

Follow this and additional works at: https://digitalcommons.csbsju.edu/honors_theses

Part of the Physics Commons

DIFFERENTIAL MODELING AND EFFICIENCY TESTING OF THE
SAINT JOHN'S UNIVERSITY COGENERATION POWER PLANT
AN HONORS THESIS
College of St. Benedict/St. John's University
In Partial Fulfillment
of the Requirements for Distinction
in the Department of Physics
by
Richard J. Kirchner
May, 2013

PROJECT TITLE: DIFFERENTIAL MODLEING AND EFFICIENCY TESTING OF THE
SAINT JOHN'S UNIVERSITY COGENERATION POWER PLANT

Approved by:

Adam Whitten

———————————————————————————
Adjunct Assistant Professor of Physics

Todd Johnson

———————————————————————————
Assistant Professor of Physics

Troy Knight

———————————————————————————
Assistant Professor of Environmental Studies

Dean Langley

———————————————————————————
Chair, Department of Physics

Anthony Cunningham

———————————————————————————
Director, Honors Thesis Program

ABSTRACT

Saint John's University (SJU) and Saint John's Abbey (SJA) of Collegeville, Minnesota own and

operate a cogeneration power plant. The produced steam serves two purposes: electricity

generation and provision of campus heat. The focus of this study was a natural gas boiler which

is the most efficient and environmentally favorable boiler in operation. Data for this study were

collected on November 8 & 9, 2012. This data set was analyzed using thermodynamic theory

which ultimately led to the determination of the efficiency of each power plant process. The

calculated efficiency values were applied to a unique set of differential equations which

accurately described power plant operation. The overall efficiency of the Saint John's University

cogeneration power plant was determined to be 73.4 ± 3.6 % which is notable in comparison to

other cogeneration facilities. Electricity generation was determined to be the least efficient

process of the power plant.

I. INTRODUCTION:

The production of steam is imperative to the generation of electricity. Generation of steam by the combustion of fossil fuel fostered the United States of America industrial revolution of the late seventeenth century by providing this nation with electrical power [Stultz & Kitto, 2005]. Modern technology has developed much further in many industries, but steam remains the largest contributor to energy production. The United States of America produced an annual total of 4095 billion kilo-watt-hours (kWh) of electricity in 2011. Of this total, 3,580 billion kWh was produced through the use of steam. This equates to approximately 90% of the nation's energy being produced by steam [USA Department of Energy, 2011]. Water/steam is used to generate electricity because it has exceptional qualities; it is a fluid that is readily available, non-toxic and well documented. These reasons support the continued election of water/steam as the fluid to produce electricity.

Steam first arrived to Saint John's University in 1909 with the construction of a cogeneration power plant [Saint John's University, 1945]. The initial power plant has seen multiple changes and renovations since the original structure was erected. The most significant change of infrastructure occurred in 1945 when SJU built and designed a new power plant [Saint John's University, 1945]. This second power plant is the structure which still stands, and houses a total of six boilers. Three different types of fuel are used by SJU to produce steam: coal, low sulfur diesel and natural gas. Of the six boilers, three burn coal, two combust low sulfur diesel fuel and the final boiler, boiler number six, combusts natural. Boiler number six is favored by the SJU power plant for its efficiency and environmental receptiveness. Since boiler number six is continuously running, it was the focus of this study. The SJU power plant also operates three

steam turbines. Average steam production only requires one of the three turbines to be running. This steam turbine is referenced as turbine number three and was the focus of this study.

The SJU power plant is unique from other power plants because it is a cogeneration facility. Cogeneration implies that the steam is assigned two uses: electricity generation and heating of campus buildings. When the natural gas fuel of boiler number six is combusted, a specific amount of heat is created. The objective of the SJU power plant is to retain the heat created by combustion and transfer it to boiler feed water. When enough heat is transferred to the feed water, it begins to boil. Additional heat is added until the water vaporizes and becomes a high pressure steam. 185 psig[1] (1.34 MPa) steam is produced by boiler number six. This steam will be referred to as high pressure (HP) steam. HP steam is transported to steam turbine number three where it is expelled over turbine blades causing them to rotate. This rotational motion is transferred to a generator which creates AC current electricity. At an average rate of 425 kilo-watts (kW), electricity generation at the power plant accounts for approximately 25 % of the campus's electrical demand [College of Saint Benedict and Saint John's University, 2013].

After generating electricity, the steam is expelled as a low pressure exhaust and serves its second purpose. This exhaust steam is a mixture of both water vapor and liquid water. The mixture exits the system at approximately 5 psig (140 kPa) and a quality of approximately 91% water vapor by mass. The remaining 9 % by mass is steam that has condensed into liquid form. This exhaust steam will be referred to as low pressure (LP) steam. The low pressure steam is transported to campus buildings where it condenses further into liquid form in small radiator units. After transferring heat to the campus buildings, the condensate returns to the power plant, completing the cycle.

---

[1] The abbreviation psig is used to indicate that the recorded value is a *gauge* pressure in units of pounds per square inch. *Absolute* pressures will be needed to accurately identify enthalpy values using steam tables. A discussion of the difference between *gauge* and *absolute* pressures is found in the *Materials and Methods* section of this report.

Saint John's University is located in Collegeville, Minnesota. It is a private catholic school with 2,000 male students. In collaboration with its sister school, The College of Saint Benedict, the pair has recently committed itself to being sustainable by initiating a sustainability program on each campus [College of Saint Benedict and Saint John's University, 2013]. An objective of this study is to complete an analysis that may supplement the sustainability of the two campuses through scientific research. Determining the efficiency of the SJU power plant will be beneficial to the university and the sustainable community it fosters.

To analyze the boiler system, methods of whole air sampling, thermodynamic analysis and differential modeling were used. Whole air sampling of the boiler exhaust was completed in collaboration with the University of California, Irvine (UCI). The Rowland-Blake Research Group at UCI is well known for its precision and accuracy in determining concentrations of trace gases in the atmosphere by collecting whole air samples [Molina & Rowland, 1974], [Simpson, Rowland, Meinardi & Blake, 2006] and [Simpson, Blake & Rowland, 2002]. The whole air sampling values of this study were used to determine efficiency of the combustion process for boiler number six. Pressure, temperature and flow rate data were collected and analyzed with methods of thermodynamic analysis to determine the efficiency of the different systems at the SJU power plant. After calculating several efficiency values for the power plant, they were incorporated into a set of differential equations to describe power plant operations. This study developed a strong foundation for future research at the SJU power plant.

III. MATERIALS AND METHODS:

This section describes the methods with which measurements of the SJU power plant were performed and how the data were used to calculate efficiency values for the power plant. This section is subdivided into eleven sections which describe the SJU power plant processes:

A. Fundamental Approach
B. Combustion
C. Heat Transfer
D. High Pressure Steam Transport
E. Electricity Generation
F. Campus Heat Provided
G. Beneficial Campus Heat
H. Condensate Collection
I. Heat Recovery – B
J. Heat Recovery – A
K. Total Plant Efficiency

Multiple physical values were measured in this experiment. Accounting for uncertainty in a measured value is imperative to conclusive scientific results:

> Experience has shown that no measurement, however carefully made, can be completely free of uncertainties. Because the whole structure and application of science depends on measurements, the ability to evaluate these uncertainties and keep them to a minimum is crucially important. – John R. Taylor [1997].

The ultimate goal of this study is to draw conclusive experimental results which include uncertainties. Appendix A is devoted to explaining the instruments and devices used to measure the physical values in this study, as well as the uncertainties associated with each of these instruments. Appendix B serves as a reference for notation used in this report.

A. Fundamental Approach

Data were collected on November 8, 2012 from 14:00 to 16:30 CST. Data recorded on November 8 was taken at a half hour frequency. Data were also collected the following day on November 9, 2012 from 10:45 to 14:00 CST. Data recorded on November 9 was taken at 15 minute intervals. After the initial data analysis, it was decided that some of the values should be

confirmed. Data were also taken on February 12, 2013 to compare with past measurements. After comparing the data sets, a final data set was constructed.

Steam engines are unique because the working substance goes through a phase transformation from liquid to vapor and back to liquid during a complete cycle. The cycle of a steam engine is best described in terms of the Rankine cycle. Description of the SJU power plant will follow the theory outlined by the Rankine cycle. This cycle has four stages, as indicated by the numbers in Figure 1. Figure 1 describes the Rankine cycle visually with a pressure vs. volume graph. Stage one of this cycle is referred to as the pump stage. This stage keeps liquid water at a constant volume while increasing its pressure. The boiler stage, stage two, adds heat to the liquid water as it flows into a boiler. This stage keeps liquid water at a constant pressure but increases its volume, causing the liquid water to become a high pressure steam vapor. Stage three is the turbine stage, which expels the high pressure steam adiabatically onto a turbine. This stage decreases the pressure of the steam and increases its volume, creating a mixture of liquid water and water vapor. The fourth stage, called the condenser stage, decreases the volume of the liquid and vapor mixture while keeping the pressure constant, returning the water to a liquid state. The cycle then repeats, beginning with the pump stage [Schroeder, 2000]. Each stage of the Rankine cycle will be explored in this study of the power plant.
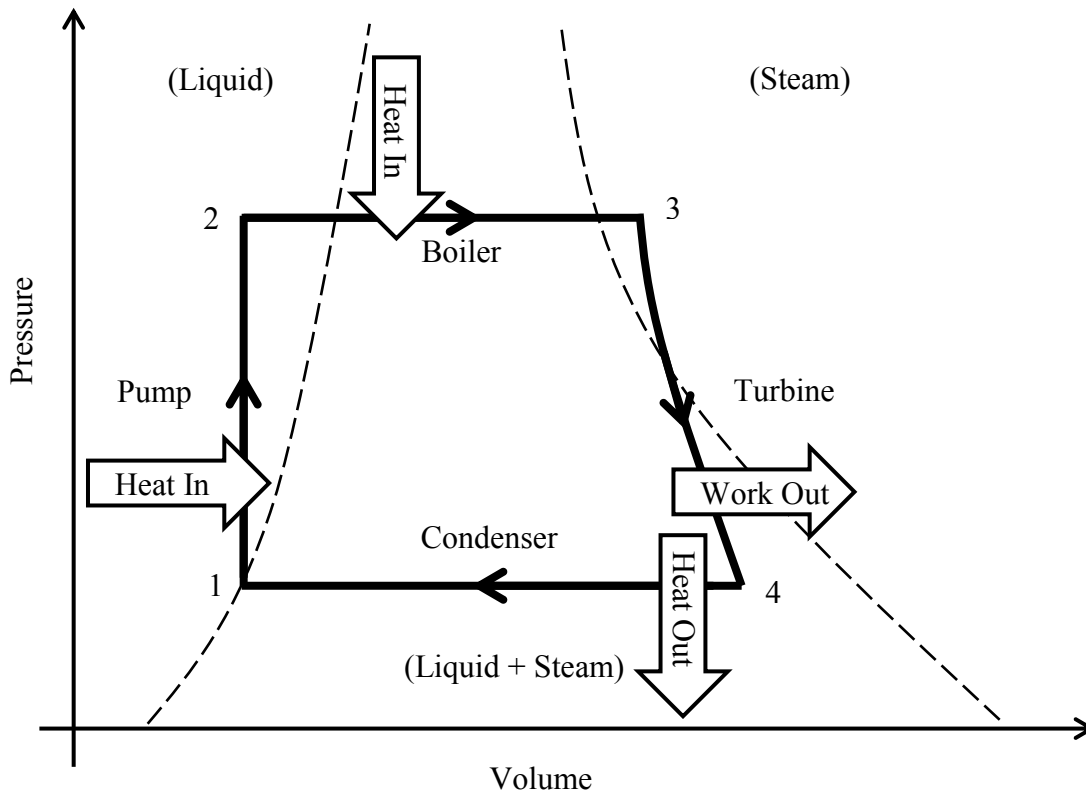
Figure 1: The ideal Rankine cycle was used to describe the SJU power plant processes. A qualitative description is provided here with a pressure vs. volume graph. The dashed lines indicate boundaries between liquid water and water vapor. The area between the dashed lines indicates water present as both a liquid and vapor. This image was **adapted from Schroeder's** *An Introduction to Thermal Physics* (2000) textbook [Schroeder, 2000].

Dr. Donald Blake, from the University of California, Irvine (UCI) provided the canisters for the whole air sampling. Dr. Blake is well known for his research in atmospheric science, especially for his methods of whole air sampling with the Rowland-Blake Research Group at UCI. Dr. Blake shipped eleven whole air sampling canisters to SJU to be used for sampling at the power plant. Samples of the natural gas boiler exhaust, as well as areas surrounding the boiler were collected for analysis.

The concentrations of methane reported from the UCI whole air sampling canisters were most applicable to this study. Natural gas has a high concentration of methane which, depending upon the quality of the fuel, may range anywhere between 70 – 95 % by volume [Naturalgas.org,

2010]. The concentration of methane in the troposphere, as of February 20, 2013 is $1.758 - 1.874$

ppmv [Blasing, 2013]. A study was conducted by the EPA to monitor the ambient indoor air of

households. This study used a threshold of 3.0 ppmv methane to commence further investigation

of methane sources in the identified household. This study also determined that any methane

concentrations exceeding 1.25 % methane by volume commenced an immediate evacuation of

household for it is indicative of the lower explosion level [Kevin, Mazzeo & Tetra, 2010]. The

same threshold values were used for this study.

Further research was performed using methods of thermodynamic analysis. Working with

the assistance of Dr. Adam Whitten, temperature, pressure and flow rate data were collected for

the different systems of the power plant. Temperatures recorded using the handheld infrared

thermometer reported the surface temperature of pipes. Since this study is concerned with the

internal temperature of the steam inside the steam pipe, a derivation for determination of this

internal temperature is given in Appendix C.

It is imperative that atmospheric pressure be determined for the SJU power plant. To

utilize steam tables for referencing enthalpy values, the pressure of a system must be expressed

as an absolute pressure. Calculating the absolute pressure is accomplished by calculating the sum

of the atmospheric and gauge pressures:

$$P_{abs} = P_{gauge} + P_{atm} \tag{1}$$

$$P_{gauge} = P_{abs} - P_{atm} \tag{2}$$

Atmospheric pressure changes with elevation. Nicholas Moe has derived the atmospheric

pressure for the elevation that corresponds to the main floor of the power plant. Moe's derivation

represents an average atmospheric pressure because some of the meters lie below the main floor

of the power plant and others are above. Moe has determined the atmospheric pressure for the

SJU power plant to be 97.061 kPa (14.3077 $psia$)[2] [Moe, 2012]. His derivation of atmospheric

pressure is shown in Appendix D. Atmospheric pressure changes temporally as well. Since

weather patterns are constantly changing, an uncertainty of 2 % was associated with the reported

atmospheric pressure value provided by Moe to account for changes in weather [NOAA, 2012].

The corrected atmospheric pressure used to calculate absolute pressure was determined to be:

$$P_{atm} = 97.1 \pm 1.9 \ kPa \tag{3}$$

A specific time interval Δt, was chosen to analysis the power plant. By choosing a specific

amount of time to analyze, specific amounts of substance flowing through the power plant such

as enthalpy, water mass and natural gas mass were determined. These data along with the

absolute pressure and temperature data were used to determine the corresponding enthalpy

values by referencing an online steam table.[3] Multiplication of the enthalpy value recorded from

a steam table, the flow rate of a substance and the time interval Δt allowed for the determination

of enthalpy values at different points in the system [Spirax Sarco, 2013]:

$$H = \frac{H}{\Delta n} \frac{\Delta n}{\Delta t} \Delta t \tag{4}$$

When referring to the enthalpy, it is important to note that the enthalpy values reported in

this study are not *absolute* values, but rather *differences* in enthalpy. This is implied and assumed

throughout the rest of this report. The reader should remind himself or herself that the enthalpy

values correspond to a change in enthalpy between different systems of the power plant.

Therefore, *H* was used to denote a change in enthalpy. This is simply a convention, and is not

intended to confuse the reader.

---

[2] The abbreviation *psia* is used to indicate that the value is an *absolute* pressure in units of pounds per square inch.
[3] The online steam table used to calculate enthalpy values for this study may be found at the following web address: http://www.spiraxsarco.com/us/resources/steam-tables.asp

Notice that both heat and work refer to energy *in transit.* You can talk about the total *energy* inside a system, but it would be meaningless to ask how much heat, or how much work, is *in* a system. We can only discuss how much heat *entered* a system, or how much work *was done on* a system – Daniel V. Schroeder [2000].

The determination of the enthalpy in each part of the system as described per equation (4) was used consistently throughout this report and allowed for comparison of enthalpy values. This process led to calculations of efficiency.

The efficiency calculations of this report do not follow conventional means of efficiency calculation. For example, conventional efficiency calculation for a heat engine is determined by the following:

$$e = \frac{W}{Q_h} \tag{5}$$

In this calculation of efficiency and W represents the work done by the system and Q_h represents the amount of heat necessary to create that amount of work. This calculation assumes that the heat expelled to the cold reservoir is wasted. For an isolated system, where the only benefit of the process is electrical work created, this sort of hot and cold reservoir approach for efficiency determination is appropriate. It is not however, a correct approach for efficiency determination of the SJU power plant. The SJU power plant is a set of integrated systems. This implies that the heat expelled into a cold reservoir in one part of the system becomes the heat provided by a hot reservoir at some point later in the system and therefore does not waste the heat.

The approach used to calculate efficiency values in this report was based on a *cost* and *benefit* analysis, which took into account that the heat expelled to a cold reservoir is not wasted:

$$e = \frac{benefit}{cost} \tag{6}$$

This approach to efficiency calculation assumes that the *cost* of the process is the amount of heat provided to the system. The *benefit* was declared to be the fraction of the provided heat that was

11

actually converted into some form of thermodynamic use which benefitted the power plant.

These efficiency calculations answer the question of: what percentage of heat provided to the

system was converted to some form of thermodynamic benefit for the system? The enthalpies at

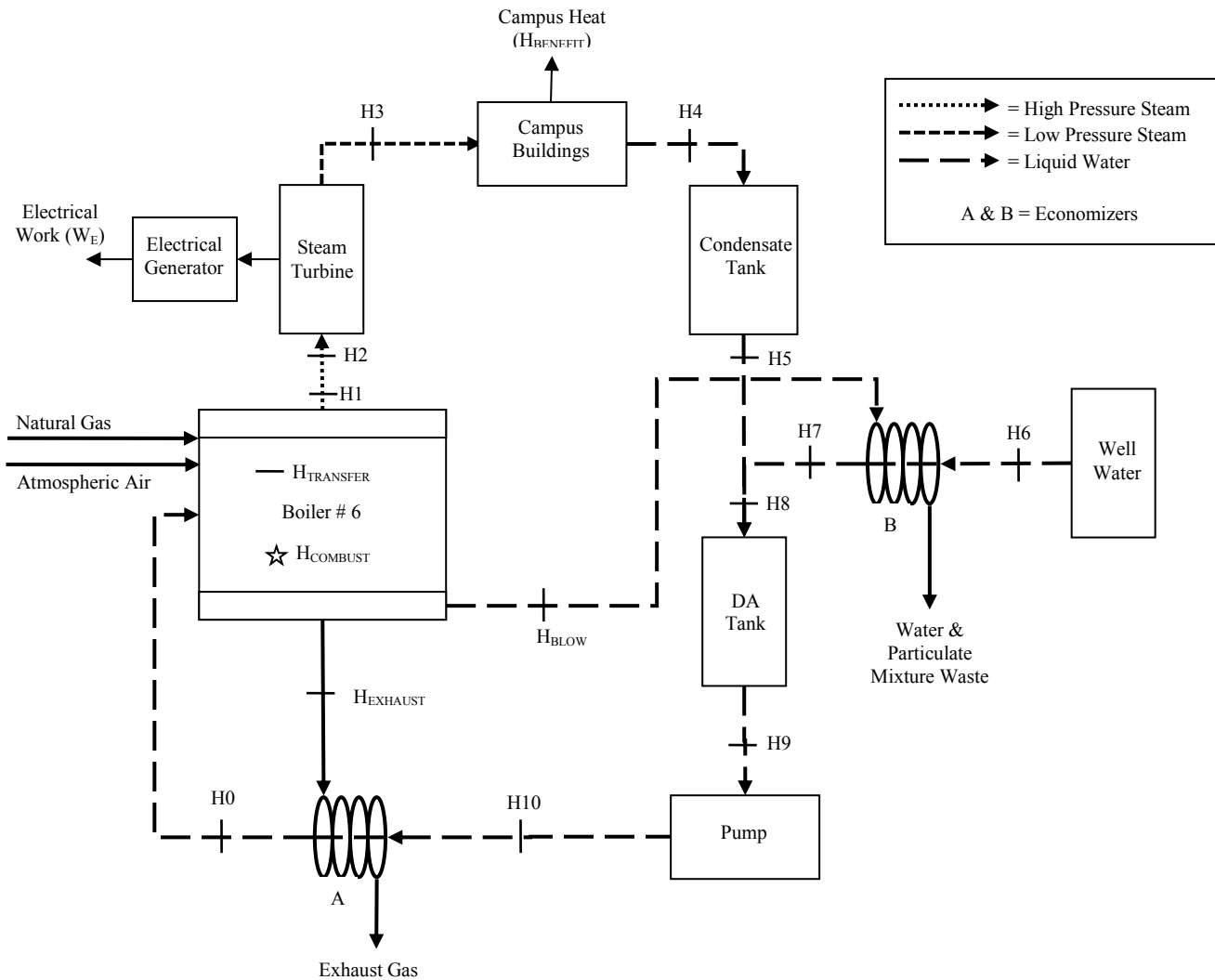different points in the cogeneration system are labeled in Figure 2.

Figure 2: **Schematic of Saint John's University's natural gas boiler (boiler # 6), and its subsystems. This figure will be continually referenced throughout the report. Gross understanding of the power plant requires the use of this schematic.**

B. Combustion

The total number of moles of natural gas that entered the combustion chamber (n_{NG}) was determined by calculating the product of the natural gas flow rate ($\Delta n / \Delta t$) and the time interval:

$$\frac{\Delta n_{NG}}{\Delta t} \Delta t = n_{NG} \tag{7}$$

The cogeneration process begins with natural gas and atmospheric air entering the combustion chamber of boiler number six. The rate of the cogeneration process is determined entirely by campus demand for heat. It is important to remind oneself of this principle when analyzing the system. The amount of heat provided to the campus is controlled manually with a throttle to constrict steam flow [Vogel, 2013]. Natural gas and air combine in a ratio that is pre-determined by a boiler engineer who adjusts mechanical valves and throttles to create the most efficient mixing ratio. This setting is checked bi-annually during state mandated boiler inspections [Vogel, 2013]. As the natural gas combusts inside the boiler, feed water enters in small pipes which outline the walls of the boiler. The feed water pipes have an outer diameter of two inches (5.08 ± 0.05 cm) and a nominal thickness of 0.210 inches (0.5334 ± 0.0053 cm).The combustion chamber of the boiler has a volume of 1084 cubic feet (30.70 ± 0.31 m^3) [Potvin, 1999]. Heat created from the combustion of natural gas and air is transferred to the feed water flowing through the boiler piping.

The flow rate of natural gas is not reported in moles per second as suggested by equation (7), but rather kilo-standard cubic feet per hour (kscfh). A standard cubic foot is measured at a temperature of 60°F and a pressure of 14.73 psi [Moe, 2012]. Converting these values to the International System of Units (SI) yields a temperature of 288.56 K and a pressure of 101.6 kPa. For this study, it was assumed that natural gas is an ideal gas. With this assumption, application

of the ideal gas law allowed for the volumetric flow rate to be converted to a molar flow rate [Schroeder, 2000]:

$$PV = nRT \tag{8}$$

$$n = \frac{PV}{RT} \tag{9}$$

$$\frac{\Delta n}{\Delta t} = \frac{P}{RT}\frac{\Delta V}{\Delta t} \tag{10}$$

By utilization of the ideal gas law, as well as proper conversion to SI units, the equation for the total number of moles of natural gas was corrected for and determined to be:[4]

$$(0.33315)\frac{\Delta V}{\Delta t[kscfh]}\Delta t = n_{NG} \tag{11}$$

To have complete understanding of the combustion process, it is necessary to account for the chemical composition of the natural gas. Different gases reactant differently with atmospheric air, and therefore create different amounts of heat when combusted. The chemical composition of the natural gas used at the SJU power plant was determined from the website of SJU's natural gas supplier, Northern Natural Gas. The chemical composition of natural gas was reported on a daily basis by Northern Natural Gas. To account for daily variation, a three month average of the natural gas was analyzed and the results are reported in Table 1 [Northern Natural Gas, 2013]:

---

[4] A full derivation of the 0.3315 factor is given in Appendix E.

Table 1: SJU natural gas chemical composition as provided by Northern Natural Gas. The reported concentrations are a three month average of daily concentration values. The reported uncertainty is the standard deviation of the three month data set:

Gas	Concentration (%)	Uncertainty (%)
Methane (CH_4)	94.6	1.3
Ethane (C_2H_6)	3.0	1.3
Nitrogen (N_2)	1.30	0.16
Carbon Dioxide (CO_2)	0.748	0.067
Other Trace Gases	0.352	0.018

The figures of Table 1 reveal that the combustion of CH_4 is most paramount to a determination of the heat created by combustion of natural gas. These figures also reveal that C_2H_6 plays a lesser, but important role in the determination of the heat created by the combustion of natural gas. Both N_2 and CO_2 do not combust with atmospheric air, so their presence is not applicable to the total amount of heat created. Finally, the amount of trace gases which compose the remainder of the natural gas was determined to be negligible in this study's calculation of the heat created by combustion of natural gas. Following the values in Table 1, the molar amounts of CH_4 and C_2H_6 were determined to be the following:
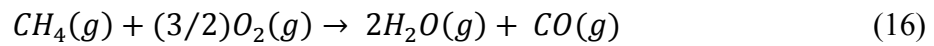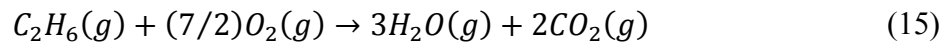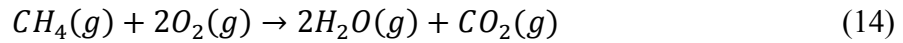
$$(0.946 \pm 0.013) * n_{NG} = n_{CH4} \tag{12}$$

$$(0.030 \pm 0.013) * n_{NG} = n_{C2H6} \tag{13}$$

There are four combustion processes that are most pertinent to this study: the combustion of CH_4 with O_2 that produces either CO_2 or CO and the combustion of C_2H_6 with O_2 that produces either CO_2 or CO. The production of CO_2 through the combustion of either CH_4 or C_2H_6 is most desirable and therefore represents most efficient combustion processes: equations (14) and (15). Production of CO_2 is most desirable because this combustion process releases the

15

most energy. The production of CO through combustion of either CH_4 or C_2H_6 is least desirable and therefore represents the least efficient combustion processes: equations (16) and (17). Production of CO is labeled as least efficient because this combustion process releases the least amount of energy. Dry atmospheric air has a chemical composition of 78% nitrogen (N_2), 21% oxygen (O_2) and 1% inapplicable trace gases by volume [McMurry & Fay, 2010]. The combustion processes used to analyze the SJU power plant are described by the following set of balanced chemical equations:

$$CH_4(g) + 2O_2(g) \rightarrow 2H_2O(g) + CO_2(g) \tag{14}$$

$$C_2H_6(g) + (7/2)O_2(g) \rightarrow 3H_2O(g) + 2CO_2(g) \tag{15}$$

$$CH_4(g) + (3/2)O_2(g) \rightarrow 2H_2O(g) + CO(g) \tag{16}$$

$$C_2H_6 + (5/2)O_2 \rightarrow 3H_2O + 2CO \tag{17}$$

The assumption was made that no liquid water was created during the combustion processes. The temperature of the combustion chamber is so great that saturation conditions have not been reached and liquid water cannot exist. This validates the assumption that no liquid water exists in the boiler exhaust gas. To determine the amount of energy each combustion process produces, the enthalpy of formation value was calculated. The enthalpy of formation for any chemical equation is given by [Schroeder, 2000]:

$$\Delta_f H = \sum n * \Delta_f H_{products} - \sum n * \Delta_f H_{reactants} \tag{18}$$

To calculate the enthalpy of formation for a given chemical reaction, it is necessary to report the standard enthalpy of formation value for each constituent molecule in the reaction. These enthalpy of formation values are well known and reported for multiple chemicals. Enthalpy of formation values for this study were recorded from the *CRC Handbook of Chemistry and Physics* and are reported in Table 2. Using relative amounts of CH_4, O_2, H_2O, CO_2 and CO,

as determined by equations (14), (15), (16) and (17), as well as their respective enthalpy of formation values from Table 2, in addition to equation (18), the enthalpy of formation per mole of CH_4 for the CO_2 and CO reaction were determined to be:

$$\Delta_f H_{CH4}(CO_2) = \left[\Delta_f H_{CO2} + 2\,\Delta_f H_{H2O}\right] - \left[2\,\Delta_f H_{O2} + \Delta_f H_{CH4}\right]$$

$$= (-802.56 \pm 3.32)\ kJ/mol$$

(19)

$$\Delta_f H_{CH4}(CO) = \left[2\,\Delta_f H_{H2O} + \Delta_f H_{CO}\right] - \left[(3/2)\,\Delta_f H_{O2} + \Delta_f H_{CH4}\right]$$

$$= (-519.58 \pm 2.67)\ kJ/mol$$

(20)

Similarly, the enthalpy of formation per mole of C_2H_6 for the CO_2 and CO reaction were determined to be:

$$\Delta_f H_{C2H6}(CO_2) = \left[2\,\Delta_f H_{CO2} + 3\,\Delta_f H_{H2O}\right] - \left[(7/2)\Delta_f H_{O2} + \Delta_f H_{C2H6}\right]$$

$$= -1428.51 \pm 5.65\ kJ/mol$$

(21)

$$\Delta_f H_{C2H6}(CO) = \left[3\,\Delta_f H_{H2O} + 2\,\Delta_f H_{CO}\right] - \left[(5/2)\,\Delta_f H_{O2} + \Delta_f H_{C2H6}\right]$$

$$= -862.55 \pm 4.05\ kJ/mol$$

(22)

Note that the enthalpy of formation values are negative. This is simply a convention which indicates that heat is extracted from the system rather than added. Taking the absolute value of each enthalpy of formation value gives the amount of heat that is produced by combustion. Also note that the enthalpy of formation values for the CO_2 reactions are larger than that of the CO reactions. This is why the CO_2 reactions are credited as most efficient.

Table 2: Enthalpy of formation values for select gases (T = 298.15 K, P = 100 kPa) [Lide, 2007]:

Gas	Enthalpy of Formation $\Delta_f H$ (kJ/mol)	CRC Unc. (kJ/mol)	0.5 % Unc. (kJ/mol)	Total Unc. (kJ/mol)
CH_4	-74.61	0.21	0.37	0.58
C_2H_6	-84.00	0.10	0.42	0.52
CO_2	-393.51	0.13	1.97	2.10
CO	-110.53	0.17	0.55	0.72
H_2O	-241.83	0.04	1.21	1.25
O_2	0.0	N/A	N/A	N/A

The values in Table 2 are reported for a specific temperature and pressure. It is correct to assume that both pressure and temperature deviations should be considered. Small deviations in pressure have negligible effects on the enthalpy of formation values. Temperature deviations have a much greater effect and were taken into consideration. If the natural gas entering the boiler has a temperature different from the standard 298.15 K, its enthalpy of formation value will also differ because more internal energy has been stored in the gas. Since the enthalpy of formation is dependent upon temperature, a new enthalpy of formation was explored. The difference between the actual enthalpy of formation and the enthalpy of formation reported at standard temperature and pressure[5] is given by the following equation [Schroeder, 2000]:

$$\Delta_f H_{Actual} - \Delta_f H_{STP} = c_{P-CH4}\Delta T = c_{P-CH4}(T_{Actual} - 298.15\ K) \qquad (23)$$

$$\Delta_f H_{Actual} = c_{P-CH4}(T_{Actual} - 298.15\ K) + \Delta_f H_{STP} \qquad (24)$$

The specific heat of CH_4 gas is $c_{P-CH4} = 35.7\ J/mol \cdot K$ [Lide, 2007]. The actual temperature of the natural gas entering the boiler did not deviate by more than 10 K from the standard temperature of 298.15 K. According to equation (24), the actual enthalpy of formation would differ from the standard enthalpy of formation by only 0.357 kJ/mol. This additional heat accounts for only 0.5% of the standard enthalpy of formation value. For this reason, it was

---

[5] This calculation assumed that the specific heat capacity was independent of temperature. It can also be shown that small temperature deviations are negligible in determining a specific heat capacity.

determined that the enthalpy of formation values reported in Table 2 were sufficient for use at the SJU power plant if this 0.5% error was added to the error reported by the *CRC Handbook of Chemistry and Physics*. Therefore the values in Table 2 include the systematic error introduced by the temperature difference from the standard value as well as the uncertainty reported by the *CRC Handbook of Chemistry and Physics*.

To calculate the total amount of enthalpy that is created by the combustion of natural gas, the amount of enthalpy created by the CO_2 and CO combustion processes for relative amounts of CH_4 and C_2H_6 was determined. A sum of these four values represents the total enthalpy formed by the combustion of natural gas. The relative amounts of enthalpy were determined by the whole air sampling values. By taking a fraction of the concentration of CO_2 to the sum of CO and CO_2 concentrations, the amount of enthalpy created by the CO_2 combustion processes was determined. A similar process was followed for CO. This process was followed for both CH_4 and C_2H_6. From the balanced chemical equations (14) and (16), it was determined that CO_2 and CO react in a 1:1 ratio with CH_4:

$$\frac{[CO_2]}{[CO] + [CO_2]} \Delta_f H_{CH4}(CO_2) = \Delta_f H_{CH4}(CO_2)_{Actual} \tag{25}$$

$$\frac{[CO]}{[CO] + [CO_2]} \Delta_f H_{CH4}(CO) = \Delta_f H_{CH4}(CO)_{Actual} \tag{26}$$

$$H_{CH4} = \Delta_f H_{CH4}(CO_2)_{actual} + \Delta_f H_{CH4}(CO)_{actual} \tag{27}$$

Note that H_{CH4} is the total amount of heat created per mole of CH_4. To calculate the total enthalpy created from combustion of CH_4, the product of H_{CH4} and n_{CH4} was determined:

$$H_{Combust-CH4} = H_{CH4} n_{CH4} \tag{28}$$

From the balanced chemical equations (15) and (17), it was determined that CO_2 and CO react in

a 2:1 ratio with C_2H_6:

$$\frac{2[CO_2]}{2[CO] + 2[CO_2]} \Delta_f H_{C2H6}(CO_2) = \Delta_f H_{C2H6}(CO_2)_{Actual} \tag{29}$$

$$\frac{2[CO]}{2[CO] + 2[CO_2]} \Delta_f H_{C2H6}(CO) = \Delta_f H_{C2H6}(CO)_{Actual} \tag{30}$$

$$H_{C2H6} = \Delta_f H_{C2H6}(CO_2)_{Actual} + \Delta_f H_{C2H6}(CO)_{Actual} \tag{31}$$

Note that H_{C2H6} is the total amount of enthalpy created per mole of C_2H_6. To calculate the total

enthalpy created from combustion of C_2H_6, the product of H_{C2H6} and n_{C2H6} was determined:

$$H_{Combust-C2H6} = H_{C2H6} n_{C2H6} \tag{32}$$

The total amount of enthalpy created from the combustion of natural gas was determined to be

the sum of the enthalpy created by the combustion of CH_4 and C_2H_6:

$$H_{Combust} = H_{Combust-CH4} + H_{Combust-C2H6} \tag{33}$$

The ideal combustion of the natural gas would produce the greatest amount of enthalpy

and would therefore not create CO. If CO is not present in the exhaust, then our equation for

$H_{Combust}$ reduces to $n_{CH4} \Delta_f H_{CH4}(CO_2) + n_{C2H6} \Delta_f H_{C2H6}(CO_2)$. Therefore, the efficiency of the

combustion process was determined to be:

$$e_{combustion(1)} = \frac{H_{Combust}}{n_{CH4} * \Delta H_{CH4}(CO_2) + n_{C2H6} * \Delta H_{C2H6}(CO_2)} \tag{34}$$

The efficiency of the combustion process was also calculated by accounting for the

physical amount of natural gas which was burned. By calculating a ratio of the amount of natural

gas burned to the amount of the natural gas initially expelled into the combustion chamber, a

second calculation of the combustion efficiency was determined:

$$e_{combustion(2)} = \frac{[Natural\ Gas]_{Burned}}{[Natural\ Gas]_{Initial}} \tag{35}$$

Two calculations of efficiency were performed for the combustion process because there are two sources of error. The first calculation concerns the percentage of heat recovered from the potential heat that could have been recovered, and the second concerns the physical burning of natural gas to see what percentage was used beneficially. This dual source for uncertainty means that efficiency values have a multiplicative effect. This efficiency calculation represents the percentage of heat that the natural gas had the potential to create:

$$e_{combustion} = e_{combustion(1)} * e_{combustion(2)} \tag{36}$$

C. Heat Transfer

The next step in determining the efficiency of the power plant system involved determining how much heat was absorbed by the feed water after the natural gas was combusted. Feed water flows into the boiler through pipes that line the walls of the boiler so that the heat created by combustion of natural gas may be transferred to it. The amount of heat transferred to the feed water by the combustion was determined by considering the heat capacity and latent heat of vaporization for the feed water:

$$H_{Transfer} = \Delta H_{FW} + \Delta H_{Vaporization-FW} + \Delta H_{HP-Steam} \tag{37}$$

The first transfer of heat occurs when the feed water is still a liquid. The amount of heat transferred to the feed water was determined by calculating the product of the mass amount of feed water, the heat capacity of feed water and the difference in temperature as the feed water goes from entering the boiler to boiling and becoming a high pressure steam.

$$\Delta H_{FW} = m_{FW}c_{P-FW}\Delta T_{FW} = m_{FW}c_{P-FW}(T_{Boil} - T_{Initial}) \tag{38}$$

Heat is absorbed by the feed water until it reaches its boiling point. The amount of heat required to vaporize the liquid feed water was determined by the latent heat of vaporization:

$$\Delta H_{Vaporization-FW} = m_{FW} L_{V-FW} \qquad (39)$$

After the liquid water has been vaporized, the steam becomes super-heated as it absorbs more heat from the combustion of natural gas. This process was described as:

$$\Delta H_{HP-Steam} = m_{HP-Steam} c_{P-HP-Steam} \Delta T_{HP-Steam}$$
$$= m_{HP-Steam} c_{P-HP-Steam} (T_{Final} - T_{Boil}) \qquad (40)$$

Therefore the total amount of combustion heat transferred to the feed water is summarized as:

$$H_{Transfer} = m_{FW} c_{P-FW}(T_{Boil} - T_{Initial}) + m_{FW} L_{V-FW}$$
$$+ m_{HP-Steam} c_{P-HP-Steam}(T_{Final} - T_{Boil}) \qquad (41)$$

The boiling point of water (T_{Boil}), the specific heat capacity of water (c_{P-FW}), the specific heat capacity of steam ($c_{P-HP-Steam}$) and the latent heat of vaporization of water (L_{V-FW}) are all dependent upon the pressure and temperature of the high pressure steam leaving the boiler system or the pressure and temperature of the feed water entering the boiler system. The absolute pressure and temperature of the high pressure steam were determined to be 1340 ± 14 kPa and 469.8 ± 7.1 K respectively. These conditions determined the boiling point of water [Lide, 2007], the specific heat capacity of steam [Steam Tables Online, 2008] and the latent heat of vaporization of water [Lide, 2007]. The absolute pressure and temperature of the feed water were determined to be 1666 ± 15 kPa and 402.0 ± 2.0 K respectively. These conditions determined the heat capacity of the feed water [Steam Tables Online, 2008]. The boiling point of water, the specific heat capacity of steam, the latent heat of vaporization of water and the specific heat capacity of the feed water were found to be:

$$T_{Boil} = 466.13 \pm 0.48 \; K^{6} \qquad (42)$$

_____

[6] A theoretical approach to determining the boiling point of water under the stated conditions would be to use the Clausius-Clapeyron equation. This approach yields a result similar to equation (33), but the result of equation (33) was determined using experimental data provided by the CRC Handbook. Therefore the reported boiling point of water is a better representation of the actual boiling point.

$$c_{P-HP-Steam} = 2.664 \pm 0.066 \; kJ/(kg \cdot K) \tag{43}$$

$$L_{V-FW} = 35.18 \pm 0.52 \; kJ/mol \tag{44}$$

$$c_{P-FW} = 4.2588 \pm 0.0039 \; kJ/(kg \cdot K) \tag{45}$$

To complete the calculation for $H_{Transfer}$, it is necessary to determine the total mass of water and high pressure steam. The mass of the high pressure steam was determined by calculating the product of the high pressure steam flow rate and the chosen time interval. Since the SJU power plant only provided records of high pressure steam flow rate, a method to determine the flow rate of feed water was developed. According to the manufacturer specification of boiler number six, 2.5% of the water that enters the boiler system exits as blow down water [Potvin, 1999]. Blow down water is removed to maintain the boiler system. By removing the blow down water from the system and discarding of the particulates it carries, the power plant is able to maintain its system more properly. Using this information, the mass amount of high pressure steam and feed water were determined to be:

$$\frac{\Delta m_{HP-Steam}}{\Delta t} \Delta t = m_{HP-Steam} \tag{46}$$

$$(1 - 0.025)m_{FW} = (0.975)m_{FW} = m_{HP-Steam} \tag{47}$$

$$m_{FW} = \left(\frac{1}{0.975}\right) m_{HP-Steam} \tag{48}$$

$H_{Transfer}$ is an expression for the amount of heat transferred to the feed water from the combustion of natural gas. The efficiency of this heat transfer process expresses the percentage of combustion heat that was transferred to the feed water and was calculated to be:

$$e_{Transfer} = \frac{H_{Transfer}}{H_{Combust}} \tag{49}$$

After the high pressure steam exits the boiler, it is transported to a steam turbine which drives an electrical generator to create electricity. This transport process allows for enthalpy loss. By determining the enthalpy value at the point where the steam leaves the boiler H_1 and contrasting it to the point where the steam enters the turbine H_2, the amount of heat lost during steam transport was determined. By recording a specific absolute pressure and temperature and referencing a steam table, the enthalpy values at points H_0 and H_2 were determined. The enthalpy at point H_1 was determined by two separate methods: (A) finding the sum of the enthalpy initially present in the feed water H_0 and the amount of heat transferred to the feed water $H_{Transfer}$ and (B) recording an absolute pressure and temperature at the point H_1 and referencing a steam table to determine the specific enthalpy for that point.

$$H_0 = \frac{\Delta H_0}{\Delta n} \Delta n_{FW} \tag{50}$$

$$H_2 = \frac{\Delta H_2}{\Delta n} \Delta n_{HP-Steam} \tag{51}$$

$$H_{1-A} = H_0 + H_{Transfer} \tag{52}$$

$$H_{1-B} = \frac{\Delta H_1}{\Delta n} \Delta n_{HP-Steam} \tag{53}$$

The reported value for H_1 was a weighted average which accounts for the reported uncertainty σ_{1-A} and σ_{1-B} of H_{1-A} and H_{1-B} respectively [Taylor, 1997]:

$$H_1 = \frac{\left(\frac{1}{\sigma_{1-A}}\right)^2 H_{1-A} + \left(\frac{1}{\sigma_{1-B}}\right)^2 H_{1-B}}{\left(\frac{1}{\sigma_{1-A}}\right)^2 + \left(\frac{1}{\sigma_{1-B}}\right)^2} \tag{54}$$

Comparison of H_1 and H_2 allowed for determination of the steam transport efficiency. This efficiency value represents the percentage of enthalpy leaving the boiler that reaches the turbine.

$$e_{Transport} = \frac{H_2}{H_1} \tag{55}$$

E. Electricity Generation

As the high pressure steam reaches the turbine, it expands and does work onto the turbine blades. The turbine work is converted to electricity by means of an AC generator. After the steam expands and does work on the turbine blades, it leaves the system as a low pressure steam which is a by-product of the electrical generation process. To determine the efficiency of this process, the enthalpy values of the high pressure steam, low pressure steam and the electrical output produced by the process were compared.

The electrical output of the generator is recorded by the SJU power plant in units of kilo-watts (kW). An important determinant in the enthalpy value of steam, besides its pressure and temperature, is its quality χ. The steam quality χ represents the fraction by mass of the total steam that is water vapor. Thus far in the analysis, it was assumed that the high pressure steam has been 100 % water vapor. The quality of the high pressure steam is actually unknown, but because it goes through a steam separator before entering the steam turbine, it was assumed that the high pressure steam has a quality of nearly 100 % ($\chi = 1 \pm 0.01$). The same is not true for the low pressure steam leaving the turbine. The absolute pressure and temperature conditions of the low pressure steam allow for the steam to be present as either a liquid or a vapor and the fraction of the two is described by the steam quality value. Nicholas Moe has determined the quality of the low pressure steam leaving the steam turbine to be [Moe, 2013]:

$$\chi = 0.905 \pm 0.039 \tag{56}$$

Moe's full derivation of steam quality is given in Appendix F of this report. It was determined that the low pressure steam leaving the turbine has a pressure of:

$$P_{LP-Steam} = 138.6 \pm 4.8 \ kPa \tag{57}$$

Utilizing the steam pressure and quality values, a specific enthalpy value was determined using a Mollier steam diagram as shown below in Figure 3:
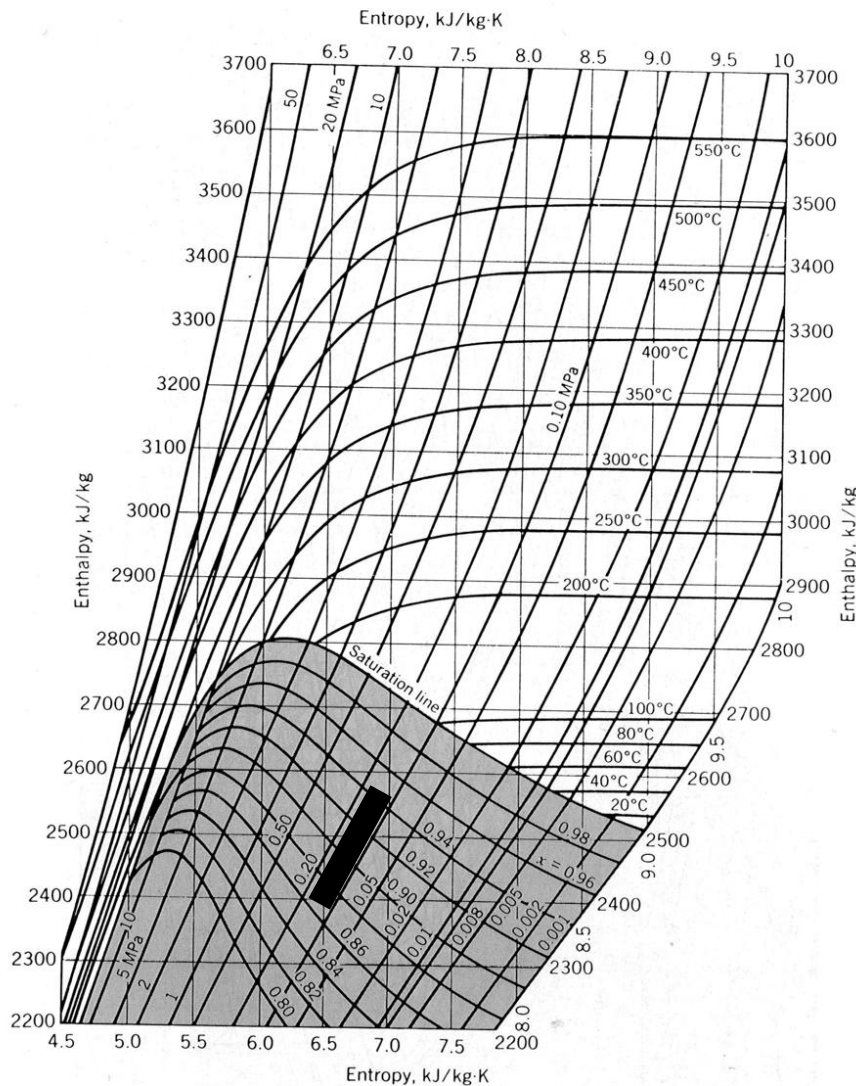

Figure 3: Mollier diagram for steam. The darkened box indicates the area in which the turbine at the SJU power plant operates. The reported specific enthalpy value is the average of the maximum and minimum specific enthalpy values. The reported uncertainty is half the difference between the maximum and minimum specific enthalpy values [Jones & Hawkins, 1986].

The specific enthalpy of steam leaving the turbine was determined using the Mollier diagram:

$$\frac{\Delta H_3}{\Delta n} = 44.6 \pm 1.6 \ kJ/mol \tag{58}$$

The total enthalpy was determined by multiplying the specific enthalpy value found from the Mollier diagram by the amount of low pressure steam:

$$m_{LP-Steam} = \frac{\Delta m_{LP-Steam}}{\Delta t} \Delta t \tag{59}$$

$$H_3 = \frac{\Delta H_3}{\Delta n} \Delta n_{LP-Steam} \tag{60}$$

The efficiency of the electrical generation process represents the percentage of heat converted to electric work of the total amount of heat provided to do so:

$$e_{Generation} = \frac{W_E}{H_2 - H_3} \tag{61}$$

To provide a comparison with power plants that are not cogeneration and only generate electricity, a conventional determination of the efficiency of the generator was also calculated which assumes that the low pressure steam is expelled as waste. This standard determination of the efficiency of the electrical generation process was referred to as $e_{Generation-Standard}$:

$$e_{Generation-Standard} = \frac{W_E}{H_2} \tag{62}$$

F. Campus Heat Provided

After the low pressure steam is expelled from the turbine, it is transported to campus buildings where it condenses into liquid water and provides heat to campus buildings. It was assumed that all of the water returning to the power plant from the campus buildings had condensed into a liquid; 100 % of the water returning is in liquid form and no steam is present.

Since little data were available for the returning condensate from campus, the assumption was made that the flow rate of the low pressure steam leaving the power plant to the campus is equal to the flow rate of condensate coming back to the power plant from campus buildings. Although some amount of water is lost during this process, the amount lost was assumed to be negligible for this study. The enthalpy at point H_4 was determined by recording an absolute pressure and temperature and referencing a steam table:

$$H_4 = \frac{\Delta H_4}{\Delta n} \Delta n_{LP-Steam} \tag{63}$$

The amount of enthalpy provided to the campus was determined by two separate methods: (A) calculating the difference in the enthalpy of the steam leaving the power plant and the enthalpy of the steam returning to the power plant and (B) looking at the amount of steam that condensed to liquid water and using specific heat capacities along with the specific latent heat of vaporization and steam quality to calculate the amount of enthalpy provided to the campus for heating.

$$H_{Provided-A} = H_3 - H_4 \tag{64}$$

$$H_{Provided-B} = \Delta H_{LP-Steam} + \Delta H_{Vaporization-CW} + \Delta H_{CW} \tag{65}$$

$$H_{Provided-B} = \chi m_{LP-Steam} c_{P-LP-Steam} \left(T_{Initial} - T_{Liquid}\right)$$
$$+ \chi m_{LP-Steam} L_{v-CW} + m_{LP-Steam} c_{P-CW} \left(T_{Liquid} - T_{Final}\right) \tag{66}$$

The reported value for $H_{Provided}$ was a weighted average which accounts for the reported uncertainty $\sigma_{Provided-A}$ and $\sigma_{Provided-B}$ of $H_{Provided-A}$ and $H_{Provided-B}$ respectively [Taylor, 1997]:

$$H_{Provided} = \frac{\left(\frac{1}{\sigma_{Provided-A}}\right)^2 H_{Campus-A} + \left(\frac{1}{\sigma_{Provided-B}}\right)^2 H_{Provided-B}}{\left(\frac{1}{\sigma_{Provided-A}}\right)^2 + \left(\frac{1}{\sigma_{Provided-B}}\right)^2} \tag{67}$$

The condensation point of water (T_{Liquid}), the specific heat capacity of the condensate water (c_{P-CW}), the specific heat capacity of the low pressure steam ($c_{P-LP-Steam}$) and the latent heat of vaporization of water (L_{V-CW}) are all dependent upon the absolute pressure and temperature of the low pressure steam leaving the steam turbine and the absolute pressure and temperature of the condensate water returning to the power plant from campus. The absolute pressure and temperature of the low pressure steam were determined to be 138.6 ± 4.8 kPa and 378.4 ± 5.7 K respectively. These conditions determined the specific heat capacity of the low pressure steam [Steam Tables Online, 2008]. The absolute pressure and temperature of the condensate water were determined to be 145.3 ± 7.3 kPa and 326.6 ± 4.9 K respectively. These conditions determined the specific heat capacity of the condensate water [Steam Tables Online, 2008], the condensation point of water [Lide, 2007] and the latent heat of vaporization of the condensate water [Lide, 2007]. The specific heat capacity of the low pressure steam, the specific heat capacity of the condensate water, the condensation point of water and the latent heat of vaporization of the condensate water were found to be:

$$c_{P-LP-Steam} = 2.27 \pm 0.10 \ kJ/(kg \cdot K) \tag{68}$$

$$c_{P-CW} = 4.182 \pm 0.010 \ kJ/(kg \cdot K) \tag{69}$$

$$T_{Liquid} = 383.5 \pm 1.5 \ K \tag{70}$$

$$L_{V-CW} = 42.77 \pm 0.36 \ kJ/mol \tag{71}$$

G. Beneficial Campus Heat

Since data were limited, two approximations, $H_{Benefit-A}$ and $H_{Benefit-B}$, were made to determine the amount of heat, $H_{Benefit}$, that is actually transferred to campus buildings to serve as a benefit. By calculating a weighted average of the two approximations, a best estimate for the amount of heat actually transferred to the campus buildings to serve as a benefit was determined.

The first approximation included many assumptions: (1) The high pressure steam piping material, including the metal pipe and insulation material, is similar to the piping material used to transport the low pressure steam to campus (2) There are 33 campus buildings which are heated by the condensation of low pressure steam (3) Each of these 33 buildings has a steam transport pipe that is separate from all other steam transport pipes (4) Each of the 33 buildings demand equal amounts of heat (5) The steam pipes used for transport take the shortest path to the building which is heated, i.e. a straight line from the SJU power plant (6) The amount of heat lost is directly proportional to the length of the steam pipe (7) The amount of heat lost during steam transport to campus is equal to the amount of heat lost during the return of condensate to the power plant.

Making these seven assumptions allows for a large introduction of error. (1) The high pressure steam piping material may be very different from the piping used to transport the low pressure steam to campus. Taking this into consideration, the percent of heat lost per meter was adjusted within plausible values to include the percent of heat lost per meter of the low pressure steam pipe. This error was included in the final uncertainty value. (2) There is no error introduced with determining the number of buildings that are heated by the low pressure steam as this should be an exact number. (3) It is likely that each of the 33 campus buildings does not have a separate transport pipe. Many of the buildings are likely located within close proximity of each other, and therefore share a steam transport pipe. If this does happen to be the case, the total distance of low pressure steam piping would decrease, and thus decrease the amount of heat lost. The total distance of the low pressure steam piping was adjusted with plausible values to include the possibility of low pressure steam pipes being daisy-chained. The error associated with this effect was included in the final uncertainty value. (4) Since each of the 33 buildings are different

30

sizes, they do not demand equal amounts of heat. For this reason, the percent of heat provided to each campus building was varied within plausible values to compensate for different demands for heat by campus buildings. This error was included in the final uncertainty value. (5) It is very likely that the low pressure steam pipes do not take the shortest route possible to the building which is being heated. The total distance of the low pressure steam piping was adjusted with plausible values to include the possibility of low pressure steam pipes not taking direct paths to the campus buildings. The error associated with this effect was included in the final uncertainty value. (6) The amount of heat lost should not be directly proportional to the amount of heat lost. If one were to examine a reasonably long pipe with this analysis, he would conclude that all the heat is lost by the time it reaches its destination. This simply cannot be true. Taking this into consideration, the percent of heat lost per meter was adjusted within plausible values to include the fact that heat lost is not directly proportional to the length of the piping. This error was included in the final uncertainty value. (7) Finally, since the amount of heat lost during steam transport to campus may not equal the amount of heat lost during steam transport back to the power plant. The steam leaving the power plant is high pressure and contains much energy which allows for more heat loss in comparison to the amount of heat lost from the return of a low pressure condensate. The amount of heat lost for the different types of steam being transported was adjusted within plausible values. Assumptions (1) through (7) amount to a total uncertainty in the amount of heat provided to the campus of 20 %.

The distance to each of the buildings was determined by using the distance measurement tool in Google Maps [Google, 2013]. Two measurements were made: the greatest possible distance between the power plant and the building of interest and the shortest possible distance between the power plant and the building of interest. An average of these distances was reported

31

as the length of the low pressure steam pipe with an uncertainty determined by half the difference between the largest and shortest distances. The determined steam pipe length was then multiplied by two to take into account steam transport to campus from the power plant, and condensate return to the power plant from campus. A table of distance values for each campus building is reported in `Appendix G`:

$$d_{LP-Pipe} = \frac{d_{High} + d_{Low}}{2} \tag{72}$$

$$\delta d_{LP-Pipe} = \frac{d_{High} - d_{Low}}{2} \tag{73}$$

$$d_{Total} = 2 * d_{LP-Pipe} \tag{74}$$

The efficiency of steam transport was previously calculated. Under the assumption that the low pressure steam transport piping is similar to that of the high pressure steam transport piping, the amount of heat lost per unit length was determined by:

$$\frac{Fraction\ Heat\ Lost}{Length\ of\ Pipe} = \frac{(1 - e_{Transport})}{d_{HP-Pipe}} \tag{75}$$

This value represents the fraction of initial heat lost per unit length of piping. Therefore, to finding the total fraction of initial heat lost, the distance of the low pressure pipe was multiplied by this value:

$$Fraction\ Heat\ Lost = \frac{(1 - e_{Transport})}{d_{HP-Pipe}} d_{Total} \tag{76}$$

Assuming that all of the campus buildings require equal amounts of heat, the amount of heat provided to each building was expressed as:

$$H_{Building} = \frac{H_{Provided}}{33} \tag{77}$$

Multiplying this value by the fraction of heat lost gives the total amount of heat that reached the campus building and provided beneficial heat:

$$H_{Benefit-A-i} = H_{Building} \frac{(1 - e_{Transport})}{d_{HP-Pipe}} d_{Total} \qquad (78)$$

Therefore, the total amount of heat provided to the campus buildings that benefitted the heating of the campus is the summation of all these enthalpy values:

$$H_{Benefit-A} = \sum_{i=1}^{33} \left[H_{Building} \frac{(1 - e_{Transport})}{d_{HP-Pipe}} d_{Total} \right]_i \qquad (79)$$

The second approximation used the property of thermal conductivity to determine the amount of heat lost during the heating of campus buildings. Heat from the steam conducts through the walls of the transport pipe and the insulation that surrounds the pipe as depicted in Figure 4. The rate of heat transferred by conduction for each of the 33 transport pipes may be determined by the following equations. Thermal conductivity $k_{Insulation}$ and the annual mean of the ground temperature T_C are reported [Young & Freedman, 2008]:

$$\frac{\Delta H_{Conduction}}{\Delta t} = k_{Insulation} A \frac{T_H - T_C}{L} \qquad (80)$$

$$k_{Insulation} = 0.0699 \pm 0.026 \ \frac{W}{m \cdot K} \qquad (81)$$

$$A = 2 * \pi * R_2 * d_{Total} \qquad (82)$$

$$T_C = 283 \pm 14 \ K \qquad (83)$$
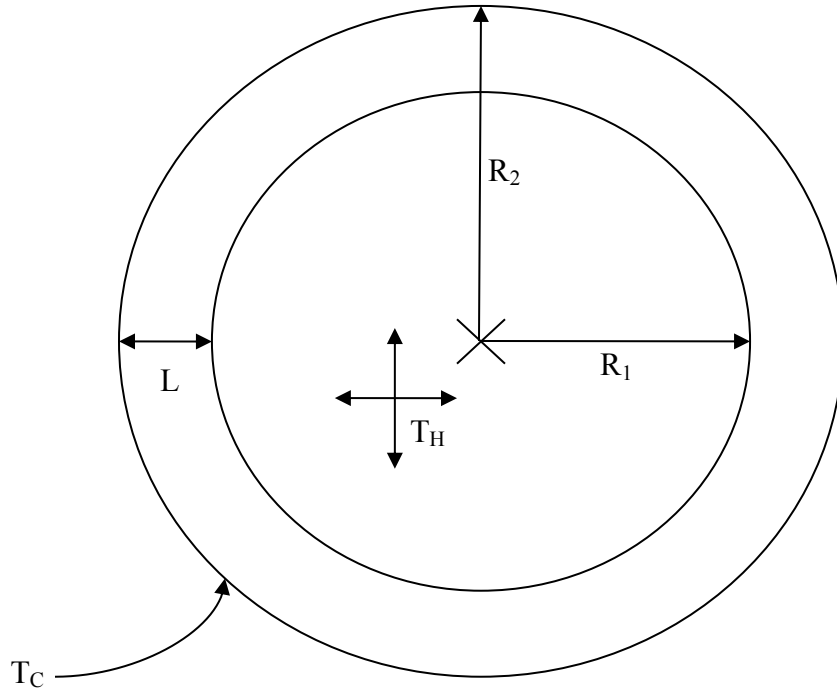
$$L = R_2 - R_1 \qquad (84)$$

Figure 4: Schematic of low pressure steam transport pipe. SJU Power Plant uses Schedule 40 steel piping for transporting steam.

Multiplying the time rate of heat conduction by the time interval gives the total amount of heat lost during low pressure steam transport:

$$\frac{\Delta H_{Conduction}}{\Delta t} \Delta t = H_{Conduction} \tag{85}$$

$H_{Conduction}$ was calculated for each of the 33 pipes. Therefore, the total amount of heat lost during heating of the campus is the summation of all these enthalpy values:

$$H_{Total\ Lost} = \sum_{i=1}^{33} [H_{Conduction}]_i \tag{86}$$

Finally, the amount of heat provided to the campus buildings that benefitted the heating of the campus was calculated using this second approximation:

$$H_{Benefit-B} = H_{Provided} - H_{Total\ Lost} \tag{87}$$

The reported value for $H_{Benefit}$ was a weighted average which accounts for the reported uncertainty $\sigma_{Benefit-A}$ and $\sigma_{Benefit-B}$ of $H_{Benefit-A}$ and $H_{Benefit-B}$ respectively [Taylor, 1997]:

$$H_{Benefit} = \frac{\left(\frac{1}{\sigma_{Benefit-A}}\right)^2 H_{Benefit-A} + \left(\frac{1}{\sigma_{Benefit-B}}\right)^2 H_{Benefit-B}}{\left(\frac{1}{\sigma_{Benefit-A}}\right)^2 + \left(\frac{1}{\sigma_{Benefit-B}}\right)^2} \tag{88}$$

The efficiency of the campus heating process may then be determined. This efficiency value represents the percentage of heat provided to the campus which was actually beneficial to campus heating:

$$e_{Campus} = \frac{H_{Benefit}}{H_{Provided}} \tag{89}$$

H. Condensate Collection

The condensate that returns from campus collects in a condensate tank. The enthalpy value of the condensate leaving the condensate tank is H_5. This water mixes with make-up water with an enthalpy value of H_7. This make up water is added to the system to compensate for the water lost through the blow down process. Since the make-up water compensates for the water loss, it was assumed that the amount of blow-down water lost is the same as the amount of make-up water added back to the system:

$$m_{BD} = (0.025)m_{FW} \tag{90}$$

$$m_{BD} = m_{MW} \tag{91}$$

H_5, H_6, and H_7 were calculated by recording a specific temperature and absolute pressure and referencing a steam table:

$$H_5 = \frac{H_5}{\Delta n}\Delta n_{LP-Steam} \tag{92}$$

$$H_6 = \frac{\Delta H_6}{\Delta n} \Delta n_{FW} \tag{93}$$

$$H_7 = \frac{\Delta H_7}{\Delta n} \Delta n_{MW} \tag{94}$$

The enthalpy at H_8 is the sum of the enthalpies H_5 and H_7:

$$H_8 = H_5 + H_7 \tag{95}$$

I. Heat Recovery - B

Since the blow down water exiting the power plant is at a significantly higher temperature than the make-up water coming from the well water, a heat recovery system (economizer) was developed by the SJU Power Plant. Rather than allowing the heated blow down water to be expelled as waste, some of the heat is transferred to the make-up water by putting the two in thermal contact. The amount of heat transferred during this process is determined by the temperature difference of the make-up water at points before it comes in thermal contact with the blow down water (H_6), and after is has absorbed some of the thermal energy (H_7). The amount of heat that was recovered from economizer B is the difference between H_7 and H_6:

$$H_{Recover-B-1} = H_7 - H_6 \tag{96}$$

The amount of heat recovered from economizer B was determined a second way by using the heat capacitance of water:

$$H_{Recover-B-2} = m_{MW} c_{P-MW} \Delta T = m_{MW} c_{P-MW} (T_7 - T_6) \tag{97}$$

The specific heat capacity of the make-up water (c_{P-MW}) is dependent upon the pressure and temperature of the make-up water coming from the well. The initial pressure and temperature of the make-up water were determined to be 517 ± 26 kPa and 283 ± 14 K

respectively. These conditions determined the heat capacity of the make-up water [Steam Tables Online, 2008]. The specific heat capacity of the make-up water was found to be:

$$c_{P-MW} = 4.186 \pm 0.010 \ kJ/(kg \cdot K) \tag{98}$$

The reported value for $H_{Recover-B}$ was a weighted average of $H_{Recover-B-1}$ and $H_{Recover-B-2}$:

$$H_{Recover-B} = \frac{\left(\frac{1}{\sigma_{Recover-B-1}}\right)^2 H_{Recover-B-1} + \left(\frac{1}{\sigma_{Recover-B-2}}\right)^2 H_{Recover-B-2}}{\left(\frac{1}{\sigma_{Recover-B-1}}\right)^2 + \left(\frac{1}{\sigma_{Recover-B-2}}\right)^2} \tag{99}$$

The enthalpy of the blow down water was determined to be:

$$H_{Blow} = \frac{\Delta H_{Blow}}{\Delta n} n_{BD} \tag{100}$$

The efficiency of economizer B was determined by a cost/benefit analysis. The benefit of this process is the heat recovered from the blow down water $H_{Recover-B}$. The cost of this process is the enthalpy of the blow down water leaving the boiler. Therefore the efficiency is an expression of the fraction of energy that the economizer extracted from the blow down water:

$$e_{Recover-B} = \frac{H_{Recover-B}}{H_{Blow}} \tag{101}$$

J. Heat Recovery - A

Feed water enters the DA tank with an enthalpy value of H_8. A DA tank works to remove oxygen and other dissolved gases that are present in the returning boiler condensate. Removal of the dissolved gases is vital for system maintenance. The presence of dissolved gases in boiler feed water such as oxygen will cause metal instruments of the boiler system to rust through formation of oxides. Dissolved gases are removed from the condensate water by the introduction of negligible amounts of low pressure steam, as well as oxygen scavenging chemicals. This process separates the dissolved gases from the water and allows them to escape through a vent at the top of the tank [Gary, 2010]. The process of de-aeration is not of importance to the

thermodynamic approach this study used. The removal of dissolved gases does not significantly change the enthalpy of the feed water. Once fully condensed, the feed water is pumped out of the tank and back into the steam boiler. Rankine cycle theory declares that pumping has negligible effect on enthalpy values of the feed water:

$$H_8 = H_9 \tag{102}$$

H_{10} was calculated by recording a specific temperature and absolute pressure and referencing a steam table:

$$H_{10} = \frac{\Delta H_{10}}{\Delta n} \Delta n_{FW} \tag{103}$$

As the feed water is pumped from the DA tank to the boiler, it passes through economizer A which allows for a heat exchange between the exhaust gas and the feed water. By putting the exhaust gas and the feed water in thermal contact with each other, heat is transferred from the high temperature exhaust to the lower temperature feed water. The amount of heat that was recovered from economizer A is the difference between H_0 and H_{10}:

$$H_{Recover-A-1} = H_0 - H_{10} \tag{104}$$

The amount of heat recovered from economizer A was determined a second way by using the heat capacity of the feed water before it enters the economizer:

$$H_{Recover-A-2} = m_{FW}c_{P-BA}\Delta T = m_{FW}c_{P-BA}(T_0 - T_{10}) \tag{105}$$

The specific heat capacity of water (c_{P-BA}) is dependent upon the pressure and temperature of the feed water before it enters economizer A. The pressure and temperature of the feed water were determined to be 1666 ± 15 kPa and 380.8 ± 2.0 K respectively. These conditions determined the heat capacity of the feed water [Steam Tables Online, 2008]. The specific heat capacity of water was found to be:

$$c_{P-BA} = 4.2246 \pm 0.0031 \ kJ/(kg \cdot K) \tag{106}$$

The reported value for $H_{Recover-A}$ was a weighted average of $H_{Recover-A-1}$ and $H_{Recover-A-2}$:

$$H_{Recover-A} = \frac{\left(\frac{1}{\sigma_{Recover-A-1}}\right)^2 H_{Recover-A-1} + \left(\frac{1}{\sigma_{Recover-A-2}}\right)^2 H_{Recover-A-2}}{\left(\frac{1}{\sigma_{Recover-A-1}}\right)^2 + \left(\frac{1}{\sigma_{Recover-A-2}}\right)^2} \tag{107}$$

The efficiency of economizer A was determined by a cost/benefit analysis. The benefit of this process is the heat recovered from the blow down water $H_{Recover-A}$. The cost of this process is the enthalpy of the exhaust gas leaving the boiler. The exhaust gas carries all the heat which wasn't absorbed by the feed water. Therefore, the difference between the heat absorbed in the combustion chamber and the heat created by combustion determines the amount of exhaust heat:

$$H_{Exhaust} = H_{Transfer} - H_{Combustion} \tag{108}$$

Therefore the efficiency is an expression of the fraction of energy that the economizer extracts from the exhaust gas:

$$e_{Recover-A} = \frac{H_{Recover-A}}{H_{Exhaust}} \tag{109}$$

K. Total Plant Efficiency

This completes the Rankine cycle for the SJU power plant. From this point, feed water enters the boiler and is heated by the combustion of natural gas. Determination of the efficiency of the entire power plant was done using a cost/benefit analysis. The cost of the processes at the power plant is the heat created by the ideal combustion of natural gas plus any enthalpy H_6 present in the make-up water which enters the boiler system. The benefit of this process is the amount of electrical work in addition to the amount of heat provided to the campus buildings. Using this approach, the efficiency of the entire system was determined to be:

$$e_{Total} = \frac{W_E + H_C}{n_{CH4}\Delta H_{CH4}(CO_2) + n_{C2H6}\Delta H_{C2H6}(CO_2) + H_6} \tag{110}$$

RESULTS:

The whole air samples were collected by the chief engineer of the power plant, Tom Vogel. Mr. Vogel collected samples of the boiler exhaust and areas where he suspected a natural gas leak on September 25, 2012. The whole air sampling canisters were returned to UCI for analysis. The returned values are reported in Table 3 below:

Table 3: Concentrations of methane, carbon dioxide and carbon monoxide gases for samples taken of boiler # 6.

Canister #	Comments	CH4 (ppmv)	CO2 (ppmv)	CO(ppbv)
8183	Upwind Power Plant	1.887 ± 0.019	376 ± 4	120 ± 1
5199	Area Around Inlet Piping # 1	3.369 ± 0.034	572 ± 6	148 ± 1
7045	Area Around Inlet Piping # 2	2.468 ± 0.025	618 ± 6	241 ± 2
6206	Exhaust Canister #1	1.790 ± 0.018	16854 ± 169	178 ± 2
6307	Exhaust Canister # 2	2.255 ± 0.023	966 ± 10	283 ± 3

Efficiency values were calculated for the combustion process using the canister values from Table 2. Absolute pressure, temperature and flow rate data were taken. The temperatures and pressures of the system remain at a constant value regardless of the flow rates. This was confirmed by comparing the uncertainties of the recorded values with the standard deviation of the set. In all cases, the uncertainty of the instrument was greater than the standard deviation. Statistically, this implies that the values remain constant for different rate of steam production.

As mentioned, the uncertainties of the recorded values were calculated for each value using the respective uncertainty as reported in Appendix B. The standard deviation of the data set was also taken and compared to the uncertainty calculated from the manufacturer's specifications. The greatest value was then taken to be the uncertainty in the recorded value. With most of the data, the manufacturer's specification provided the greatest uncertainty value. The uncertainty value for each data point was then averaged and reported as the final uncertainty in the measured value. The final reported value is an average of all the data recorded for that specific value. A summary of the pressures and temperatures of the power plant are reported in Table 4

.

Table 4: Temperature and pressure data of the SJU power plant with respective uncertainties. The enthalpy value that follows each measured quantity indicates the place where those data were collected. Refer to Figure 2 for a reference of the location of the data recording locations.

Measured Quantity	Value	Uncertainty
Atmospheric Pressure (kPa)	97.1	1.9
Economizer A Inlet Exhaust Gas Temp-$H_{EXHAUST}$ (K)	473.8	2.6
Economizer A Outlet Exhaust Gas Temp (K)	397.7	2.0
Economizer A Inlet Water Temp-H_{10} (K)	380.8	2.0
Economizer A Outlet Water Temp-H_0 (K)	402.0	2.0
Feed Water Pressure-H_0 (kPa)	1666	15
Temp Steam Pipe-H_1 (K)	469.8	7.1
Steam Pressure-H_1 (kPa)	1340	14
Room Temp-AB (K)	309.6	2.1
Temp Steam Pipe-H_2 (K)	466.0	7.0
Steam Pressure-H_2 (kPa)	1444	14
Room Temp-AT (K)	298.6	2.0
Temp Steam Pipe-H_3 (K)	378.4	5.7
Steam Pressure-H_3 (kPa)	138.6	4.8
Pipe Temp-H_4 (K)	326.6	4.9
Condensate Pressure-H_4 (kPa)	145.3	7.3
Temp Condensate Tank-H_5 (K)	330.4	2.0
Pressure Condensate Tank-H_5 (kPa)	262	13
Temp Make-Up Water Initial-H_6 (K)	283	14
Pressure Make-Up Water-H_6 (kPa)	614	31
Temp Make-Up Water Final-H_7 (K)	369.8	1.0
Pressure Make-Up Water Final-H_7 (kPa)	614	31
Final Waste Water Temp (K)	374.3	1.0
Temp Blow Down-H_{Blow} (K)	415	21
Pressure Blow Down-H_{Blow} (kPa)	614	31
Temp DA-H_9 (K)	381.5	1.0
Pressure DA-H_9 (kPa)	125.36	0.80

The data from Table 4 was used to calculate enthalpy values for the SJU power plant. These

values are reported in Table 5.

Table 5: Enthalpy values and other pertinent data used to determine efficiency values. Data was recorded over a three hour time period; $\Delta t = 3\ hours$.

Calculated Quantity	Reported Value
$\Delta t\ (hours)$	3.00 ± 0.03
$n_{NG}\ (moles)$	$(77.0 \pm 2.3) \times 10^3$
$n_{CH4}\ (moles)$	$(72.8 \pm 2.4) \times 10^3$
$n_{C2H6}\ (moles)$	$(2.3 \pm 1.0) \times 10^3$
$n_{FW}\ (moles)$	$(1.386 \pm 0.042) \times 10^6$
$n_{LP}\ (moles)$	$(1.351 \pm 0.041) \times 10^6$
$n_{HP}\ (moles)$	$(1.351 \pm 0.041) \times 10^6$
$n_{BD}\ (moles)$	$(0.0347 \pm 0.0011) \times 10^6$
$n_{MW}\ (moles)$	$(0.0347 \pm 0.0011) \times 10^6$
$H_0\ (J)$	$(13.54 \pm 0.46) \times 10^9$
$\Delta_f H_{CH4}(CO)\ (kJ/mol)$	519.58 ± 2.67
$\Delta_f H_{CH4}(CO_2)\ (kJ/mol)$	802.56 ± 3.32
$\Delta_f H_{C2H6}(CO)\ (kJ/mol)$	862.55 ± 4.05
$\Delta_f H_{C2H6}(CO_2)\ (kJ/mol)$	1428.51 ± 5.65
$H_{Combust}\ (J)$	$(61.8 \pm 2.5) \times 10^9$
$\Delta H_{FW}\ (J)$	$(6.82 \pm 0.30) \times 10^9$
$\Delta H_{Vaporization-FW}\ (J)$	$(48.7 \pm 1.6) \times 10^9$
$\Delta H_{HP-Steam}\ (J)$	$(0.2380 \pm 0.0093) \times 10^9$

$H_{Transfer}$ (J)	$(55.8 \pm 1.6) \times 10^9$
H_{1-A} (J)	$(69.34 \pm 1.3) \times 10^9$
H_{1-B} (J)	$(68.1 \pm 1.8) \times 10^9$
H_1 (J)	$(68.7 \pm 1.4) \times 10^9$
H_2 (J)	$(67.9 \pm 2.1) \times 10^9$
W_E (J)	$(3.579 \pm 0.032) \times 10^9$
H_3 (J)	$(60.3 \pm 2.8) \times 10^9$
$\Delta H_{LP-Steam}$ (J)	$(0.054 \pm 0.001) \times 10^9$
$\Delta H_{Vaporization-CW}$ (J)	$(52.3 \pm 2.8) \times 10^9$
ΔH_{CW} (J)	$(5.79 \pm 0.16) \times 10^9$
$H_{Provided-A}$	$(54.8 \pm 2.4) \times 10^9$
$H_{Provided-B}$	$(58.1 \pm 1.9) \times 10^9$
$H_{Provided}$	$(56.4 \pm 2.0) \times 10^9$
$H_{Benefit-A}$ (J)	$(40.6 \pm 8.1) \times 10^9$
$H_{Benefit-B}$ (J)	$(43.3 \pm 9.3) \times 10^9$
$H_{Benefit}$ (J)	$(41.7 \pm 8.5) \times 10^9$
H_4 (J)	$(5.45 \pm 0.51) \times 10^9$
H_5 (J)	$(5.84 \pm 0.27) \times 10^9$
H_6 (J)	$(26.2 \pm 1.6) \times 10^9$
H_7 (J)	$(0.253 \pm 0.015) \times 10^9$
H_8 (J)	$(6.09 \pm 0.27) \times 10^9$

H_9 (J)	$(6.09 \pm 0.27) \times 10^9$
H_{10} (J)	$(11.31 \pm 0.67) \times 10^9$
H_{Blow} (J)	$(0.374 \pm 0.022) \times 10^9$
$H_{Exhaust}$ (J)	$(5.95 \pm 0.29) \times 10^9$
$H_{Recover-B-1}$ (J)	$(0.2265 \pm 0.0089) \times 10^9$
$H_{Recover-B-2}$ (J)	$(0.2268 \pm 0.0075) \times 10^9$
$H_{Recover-B}$ (J)	$(0.2266 \pm 0.0099) \times 10^9$
$H_{Recover-A-1}$ (J)	$(2.23 \pm 0.15) \times 10^9$
$H_{Recover-A-2}$ (J)	$(2.23 \pm 0.12) \times 10^9$
$H_{Recover-A}$ (J)	$(2.23 \pm 0.13) \times 10^9$

The values of Table 5 were used to calculate the efficiency values for different sub systems of the power plant using the theory described. The error was propagated through the calculations to incorporate a final error in the efficiency value. The final efficiency calculations are shown in Table 6.

Table 6: Final efficiency calculations for the SJU power plant.

Process	Efficiency (%)	Uncertainty (%)	Final Range (%)
$e_{Combustion}$	99.9	5.6	94.3 – 100
$e_{Transfer}$	90.4	4.5	85.9 – 94.9
$e_{Transport}$	98.8	3.7	95.1 – 100
$e_{Generation}$	46.72	0.60	46.12 – 47.32
$e_{Generation-Standard}$	5.94	0.47	5.47 – 6.41
e_{Campus}	74	15	59 – 89
$e_{Recover-B}$	60.6	4.4	56.2 – 65.0
$e_{Recover-A}$	37.6	2.4	35.2 – 40.0
e_{Total}	73.4	3.6	69.8 – 77.0

With the efficiency values all calculated, they may be applied to a set of differential equations to continuously describe the state of the SJU power plant. Development of a set of differential equations will allow further research at the SJU power plant to be accomplished more quickly and efficiently. This set of differential equations may also be used to create a computer model of the power plant.

The development of a set of differential equations is similar to the approach used to calculate the efficiency of each power plant subsystem. Since the power plant processes have already been described in great detail in the Materials and Methods section of this report, only the differential equations are presented:

$$\frac{dH_0}{dt} = \frac{dH_0}{dt}\frac{dn_{FW}}{dt} = \left(\frac{1}{0.975}\right)\frac{dH_0}{dt}\frac{dn_{HP-Steam}}{dt} \tag{111}$$

$$e_{Combustion(1)}\left(\frac{dn_{CH4}}{dt}\Delta H_{CH4}(CO_2) + \frac{dn_{C2H6}}{dt}\Delta H_{C2H6}(CO_2)\right) = \frac{dH_{Combust}}{dt} \tag{112}$$

$$\frac{dH_{Transfer}}{dt} = \frac{dm_{FW}}{dt}c_{P-FW}(T_{Boil} - T_{Initial}) + \frac{dm_{FW}}{dt}L_{V-FW}$$
$$+ \frac{dm_{HP-Steam}}{dt}c_{P-HP-Steam}(T_{Final} - T_{Boil}) \tag{113}$$

$$e_{Transfer}\left(\frac{dH_{Combust}}{dt}\right) = \frac{dH_{Transfer}}{dt} \tag{114}$$

$$\frac{dH_1}{dt} = \frac{dH_{Transfer}}{dt} + \frac{dH_0}{dt} = \frac{dH_1}{dn}\frac{dn_{HP-Steam}}{dt} \tag{115}$$

$$\frac{dH_2}{dt} = \frac{dH_2}{dn}\frac{dn_{HP-Steam}}{dt} \tag{116}$$

$$e_{Transport}\left(\frac{dH_1}{dt}\right) = \frac{dH_2}{dt} \tag{117}$$

$$\frac{dH_3}{dt} = \frac{dH_3}{dn}\frac{dn_{LP-Steam}}{dt} \tag{118}$$

$$e_{Generation}\left(\frac{dH_2}{dt} - \frac{dH_3}{dt}\right) = \frac{dW_E}{dt} \tag{119}$$

$$\frac{dH_4}{dt} = \frac{dH_4}{dn}\frac{dn_{LP-Steam}}{dt} \tag{120}$$

$$\frac{dH_{Provided}}{dt} = \frac{dH_3}{dt} - \frac{dH_4}{dt} \tag{121}$$

$$\frac{dH_{Provided}}{dt} = \chi\frac{dm_{LP-Steam}}{dt}c_{P-LP-Steam}(T_{Initial} - T_{Liquid})$$
$$+ \chi\frac{dm_{LP-Steam}}{dt}L_{v-CW} + \frac{dm_{LP-Steam}}{dt}c_{P-CW}(T_{Liquid} - T_{Final}) \tag{122}$$

$$\frac{dH_{Benefit}}{dt} = \frac{dH_{Provided}}{dt} - \frac{dH_{Total\ Lost}}{dt} \tag{123}$$

47

$$e_{Campus} \frac{dH_{Provided}}{dt} = \frac{dH_{Benefit}}{dt} \tag{124}$$

$$\frac{dH_5}{dt} = \frac{dH_5}{dn} \frac{dn_{LP-Steam}}{dt} \tag{125}$$

$$\frac{dH_6}{dt} = \frac{dH_6}{dn} \frac{dn_{MW}}{dt} \tag{126}$$

$$\frac{dH_7}{dt} = \frac{dH_7}{dn} \frac{dn_{MW}}{dt} \tag{127}$$

$$\frac{dH_8}{dt} = \frac{dH_5}{dt} + \frac{dH_7}{dt} \tag{128}$$

$$\frac{dH_{Recover-B}}{dt} = \frac{dH_7}{dt} - \frac{dH_6}{dt} = \frac{dm_{MW}}{dt} c_{P-MW}(T_7 - T_6) \tag{129}$$

$$\frac{dH_{Blow}}{dt} = \frac{dH_{Blow}}{dn} \frac{dn_{BD}}{dt} \tag{130}$$

$$e_{Recover-B} \left(\frac{dH_{Blow}}{dt} \right) = \frac{dH_{Recover-B}}{dt} \tag{131}$$

$$\frac{dH_8}{dt} = \frac{dH_9}{dt} \tag{132}$$

$$\frac{dH_{10}}{dt} = \frac{dH_{10}}{dn} \frac{dn_{FW}}{dt} \tag{133}$$

$$\frac{dH_{Recover-A}}{dt} = \frac{dH_0}{dt} - \frac{dH_{10}}{dt} = \frac{dm_{FW}}{dt} c_{P-BA}(T_0 - T_{10}) \tag{134}$$

$$\frac{dH_{Exhaust}}{dt} = \frac{dH_{Transfer}}{dt} - \frac{dH_{Combustion}}{dt} \tag{135}$$

$$e_{Recover-A} \left(\frac{dH_{Exhaust}}{dt} \right) = \frac{dH_{Recover-A}}{dt} \tag{136}$$

$$e_{Total} \left(\frac{dn_{CH4}}{dt} * \Delta H_{CH4}(CO_2) + \frac{dn_{C2H6}}{dt} * \Delta H_{C2H6}(CO_2) \right) = \frac{dW_E}{dt} + \frac{dH_C}{dt} \tag{137}$$

DISCUSSION:

The whole air samples for canister # 5199 and # 7045 showed a relatively large increase from the background methane value given by canister # 8183. Canisters # 5199 and # 7045 were used to sample the natural gas piping for boiler # 6. This sampling was done to check for leaks in the piping. Canister # 8183 was taken outside of the power plant to provide a background figure for the concentration of methane. The methane concentrations for cans # 8183, # 5199 and # 7045 are reported in Table 3 as: 1.887 ± 0.019 ppmv, 3.369 ± 0.034 ppmv and 2.468 ± 0.025 respectively. The places where canisters # 5199 and # 7045 were sampled therefore show an increase in methane of 78.5 ± 2.8 % and 30.8 ± 2.3 % respectively. This would seem to be a reason for concern, especially the nearly 80% increase in methane gas concentration.

Canister # 5199 exceeded the 3.0 ppmv threshold. This indicates that further investigation should be performed to possibly locate a gas leak. The reported percentage increases for canisters # 5199 and # 7045 are somewhat misleading. The concentration of methane in a given volume, such as the power plant in this study, depends heavily on the exchange rate of air in the system. Since the power plant is an enclosed space, there is not a continuous exchange of air as there is outside of the power plant. This may result in a small accumulation of methane gas. Also, the canisters were sampled directly next to the natural gas piping. If natural gas were leaking from the pipe, it would take a while to diffuse through the room. If there was a significant leak, the concentration of methane gas should be largest directly by the piping. A quick look at the number suggests that a methane gas concentration of 3.369 ± 0.034 ppmv is not a large enough anomaly for concern. Therefore no leaks in the natural gas piping were determined.

It was found that the total efficiency of the SJU power plant is 73.4 $\pm$ 3.6 %. This value seems to be fairly large for a boiler system. However, since the SJU power plant is a cogeneration facility, the total efficiency is expected to exceed that of traditional power plants which don't make use of the turbine exhaust. Similar cogeneration facilities have efficiencies of: 79 %, 78 % and 70 % [USA Department of Energy, 2000], [University of Michigan, 2010] and [Architect of the Capitol, 2013]. The most efficient cogeneration plants have efficiencies of greater than 90 % [Intelligen, 2010]. It is observed that the SJU power plant has a similar efficiency as other cogeneration plants and does not exceed the efficiency value of the most modern plants.

Calculation of $e_{Generation-Standard}$ showed that if the SJU power plant were only producing electricity and not heating campus buildings, it would have an efficiency somewhere between 5.47 – 6.41 %. This calculation displays the inefficiency of the power generation process at SJU. The power plant would certainly benefit from updating its steam turbine to one that is more efficient. This would allow for the SJU power plant to produce more power domestically while still heating the campus at the same rate.

The theory of efficiency determination should be validated with future research projects. Many of the assumptions made were gross approximations, but they were justified in each sense. Therefore, further metering and data recording of steam flow rates and similar values would allow for a better determination of the total efficiency of the system.

The combustion process had a very large efficiency value. The efficiency was nearly 100%. This is to be expected. This percentage implies that nearly 100% of the natural gas that is injected into the combustion chamber is combusted and converted to heat. The efficiency of the thermal absorption process by the steam was also found to exhibit a significantly high efficiency

of 90%. This implies that 10% of the heat that was created during the combustion process, was not transferred to the steam, but lost to the surrounding environment.

It was found that the efficiency of steam transport from the boiler to the turbine is very high. Nearly 100% of the heat which leaves the boiler reaches the turbine to be converted to electrical energy. The electrical generation process is easily the least efficient. It was found that the generator and turbine combination have an efficiency of 46.72 ± 0.60 %. This percentage implies that 47.75% of the heat which was supplied to the generator was converted to electrical work. The rest was lost to the surrounding environment. Since this process is the least efficient of all the processes, the power plant would benefit greatly from updating their electrical generators. If their generators were updated, the efficiency of the entire process would increase.

The heat recovery systems were found to have an efficiency of 60.6 ± 4.4 % and 37.6 ± 2.4 % for heat recovery systems B and A respectively. These values indicate that the reported percentage is the percentage of heat extracted from the waste fluid (either water or exhaust). It would be impossible to extract all of the thermal energy from these waste substances, and since the processes are extracting heat from water and exhaust that had been previously disposed without recovering heat, it is important to understand that they are performing well and recovering some of the heat.

Even though some of the efficiency values need to be corrected by further data collection, the set of differential equations accurately describes the system. This set of differential equations is ready to be applied to a model and create a visual description of the power plant.

CONCLUSIONS:

Canisters # 5199 and # 7045, which were used to sample the inlet piping of natural gas, did not show a significant increase in the concentration of natural gas when compared to the

background whole air sample of methane (canister # 8183). It was concluded that the areas of suspected leaks may be disregarded as reason for loss of natural gas due to inlet piping assembly. The theory for determining efficiency values should be validated with future research and corrected for if mistakes are found. The least efficient process of the power plant is electrical generation. The power plant would benefit from updating their steam turbines. The set of differential equations used to describe the processes of the power plant may be easily applied to a model. Through use of the coupled differential equations and the efficiency values, one is able to figure out the heat flow rate of parts in the system. A very solid thermodynamic foundation has been established for future research at the SJU power plant. There are many areas of future research that may occur at the SJU power plant.

ACKNOWLEDGMENTS:

APPENDICES:

APPENDIX A: Instruments and Uncertainties

To calculate uncertainties in calculated values, the following general formula was used:

$$\delta q = \sqrt{\left(\frac{\partial q}{\partial x}\delta x\right)^2 + \cdots + \left(\frac{\partial q}{\partial z}\delta z\right)^2} \qquad (138)$$

Where x,…, z are measured physical values with respective uncertainties of δx,…, δz. These measured values are used to compute a value q(x,…, z). Note that $\frac{\partial q}{\partial x}$ denotes the partial derivative of the function q with respect to x, and similarly for other measured values [Taylor, 1997].

This appendix includes a discussion of how the uncertainties for the measured values were obtained. Table 7 lists the physical value measured at the power plant, and the instrument used to record this value. Table 8 is an expansion of Table 7, which includes a column of how the uncertainties of these measured values were calculated.

Table 7: Physical value measured and the instrument which measured it:

Physical Value	Instrument Used
CH_4 Concentration	Gas Chromatographer – Flame Ionization
CO Concentration	Gas Chromatographer – Flame Ionization
CO_2 Concentration	Gas Chromatographer – Thermal Conductivity
Steam Flow Rate to Turbine	Orifice-Plate Flow Meter
Gas Flow Rate	Orifice-Plate Flow Meter
Steam Flow Rate to Campus	Prowirl 73 Meter
HP Steam Pressure	Ashcroft Duragauge – 0 psig to 300 psig
Feed Water Pressure	Ashcroft Duragauge – 0 psig to 300 psig
LP Steam Pressure	Ashcroft Duragauge – 0 psig to 15 psig
DA Tank Pressure	Ashcroft Duragauge – 0 psig to 15 psig
Surface Temperature of Steam Pipes	Fluke 62 Mini IR Thermometer
DA Tank Temperature	Alcohol Thermometer
Ambient Air Temperature	Omega Digital Thermometer (HH-25KC) – Type K
Feed Water Temperature	Yokogawa Temperature Input Meter - Thermocouple
Exhaust Gas Temperature	Yokogawa Temperature Input Meter - Thermocouple
Temperature Condensate Tank	Ashcroft Bimetal Thermometer
Temperature of Make-up Water	Trerice dial thermometer from 30-300 F
Rate of Energy Production	Crompton Switchboard Integra-Model 1540

The concentrations of gases in the whole air sampling canisters were determined using the method of gas chromatography. This method determined the concentration of methane gas (CH_4), carbon monoxide gas (CO), and carbon dioxide gas (CO_2). The whole air sampling at the SJU power plant was completed by filling evacuated air canisters with boiler exhaust gas. The canisters filled with boiler exhaust until they reached atmospheric pressure, and were then quickly sealed with the attached bellows valve. The canisters provided by UCI are two liters in volume, electropolished, constructed from stainless steel and equipped with a stainless steel Swagelok® Nupro bellows valve. The canisters were evacuated for 24 hours by means of a pump-and-flush procedure. After pumping and flushing the canisters with ambient air, the canisters were pressurized to 1000 Torr with ultra-high purity helium before a final evacuation to 10^{-2} Torr (1 Pa) [Simpson et al., 2010].

The method used for determining the concentration of the three gases varies. The gas chromatographer which measures the concentration of CH_4 uses flame ionization detection. The flame ionization detector uses combustion techniques to determine the concentration of CH_4, and is therefore destructive to the sample being measured. CH_4 is combusted with a carrier gas (H_2). The combustion process creates a group of anions. This group is proportional to the concentration of CH_4. These anions are collected on an anode and the potential difference between the cathode and anode is measured. This difference is used to determine the relative amount of CH_4 in the sample [Karmen & Haut, 1973]. The gas chromatographer that measures concentrations of CO also uses methods of flame ionization. UCI reports an uncertainty of $\pm$ 1% of the recorded value for flame ionization detection [Simpson et al., 2006].

CO_2 is measured by methods of thermal conductivity. Thermal conductivity detection is a non-destructive method which measures the difference in the thermal conductivity of a reference gas and the sampled gas. By the use of Fourier's Law, which determines the thermal conductivity of a sample, the electrical resistance of the sampled gas can be compared to the electrical resistance of the reference gas. This process ultimately determines the concentration of CO_2 [Kebbekus et al., 1965]. UCI reports an uncertainty of $\pm$ 1% of the recorded value for this method of analysis [Simpson et al., 2006].

The steam flow rate from the boiler to the turbine is measured with an orifice plate flow meter. The steam flows through a restriction called an orifice plate. The restriction creates a pressure differential across the orifice plate. The meter works on the basis of Bernoulli's Equation which relates the velocity of a fluid passing through an orifice to the pressure differential across the orifice. Correct installation of a steam plate orifice meter allows for an uncertainty in the recorded measurement of $\pm$ 3% of the recorded value [Steven & Hall, 2009].

An orifice plate meter is also used to measure the gas flow rate. Therefore the uncertainty in the recorded values for the gas flow rate is also ±3% of the recorded value.

The steam flow rate to the campus is measured with a set of Prowirl 73 vortex flow meters. These meters create small vortices in the steam by inserting a small barrier in the steam flow. The vibrating frequency of the vortices is related to the velocity of the fluid flow and ultimately a mass flow rate. The Prowirl 73 vortex flow meters used in the power plant have an uncertainty of ± 2.3% [Andress & Hauser, 2011].

All of the pressure gauges in the SJU power plant are Ashcroft Duragauge pressure gauges. The Duragauge manual reports an uncertainty of 0.5% of the recorded value. It should also be taken into consideration the graduation of the gauges. The pressure gauges used to measure high pressure steam values have a range of 0 psig to 300 psig. The Duragauge manual specifies that a gauge with this range has a minor graduation of 2 psig [Aschcroft, 2009]. This implies that the uncertainty of reading the analog scale is ± 1 psig. Therefore the uncertainty for the high pressure gauges is the sum of 1 psig and 0.5% of the recorded value. Note that the reported uncertainty for the pressures is due to both systematic and random error. The systematic error is accounted for with the 0.5% value and the random error is accounted for with the ± 1 psig value. Since there are two forms of error, the total error is assigned to be the sum of the systematic and random error. The pressure gauge used to measure the pressure of the feed water is the same model as the one used to measure the high pressure steam. For this reason, it was assigned the same uncertainty value.

The pressure gauges used to measure the low pressure steam values have a range of 0 psig to 15 psig. The Duragauge manual specifies that a gauge with this range has a minor graduation of 0.1 psig [Aschcroft, 2009]. This implies that the uncertainty of reading the analog

scale is $\pm$ 0.05 psig. Therefore the uncertainty for the low pressure gauges is the sum of 0.05 psig and 0.5% of the recorded value. Note that, similar to the error calculation for the high pressure steam measurement, the uncertainty of the low pressure steam measurement is due to both systematic and random error. The pressure gauge used to measure the pressure of the deaerator (DA) tank is exactly the same as the ones used to measure low pressure steam, so it was assigned the same uncertainty. The DA tank serves to remove oxygen and other dissolved gases in the feed water. The DA tank is used to increase the quality of feed water before it enters the boiler system.

To measure the surface temperature of the steam pipes at the power plant, the engineers use a Fluke 62 Mini infrared thermometer. This thermometer is a hand held device which uses a small laser to locate a surface of interest. The temperature of the surface is displayed as a digital value on a small screen. The device deduces a temperature by measuring a fraction of the thermal radiation emitted by the object being measured. The thermal radiation of the object being measured is focused onto a detector, which creates an electrical signal. By measuring the amount of thermal energy emitted, in combination with the object's emissivity, the Fluke 62 Mini device is able to calculate a temperature and display it on its digital screen. The device is useful for taking temperature readings in hard to reach places such as the steam piping of the SJU power plant. The Fluke 62 Mini infrared thermometer has a temperature range of 243.15 K to 773.15 K. The device assumes an ambient temperature of 296.15 $\pm$ 2 K. The device also assumes an emissivity of $\varepsilon = 0.95$. The spectral response of the device is 6.5 to 18 microns. The accuracy of the device is defined differently for different temperature ranges. According to the owner's manual, the temperature values in the range of 283.15 K to 303.15 K, have an uncertainty of $\pm$ 1 K. The manual also specifies that temperature values outside of the 283.15 K to 303.15 K range,

have an uncertainty of ± 1.5 K, or ± 1.5% of the reading, whichever is greatest [Fluke Corporation, 2008].

The temperature of the DA tank is monitored using an alcohol thermometer. Alcohol thermometers are used for measurements that don't require precision much greater than a few degrees. The minor graduations of the thermometer are 1 degree Fahrenheit. Therefore it was assumed that the uncertainty in the alcohol thermometer reading is ± 1 degree Fahrenheit.

An Omega Digital Thermometer model HH-25KC was used to record ambient air temperature. The Thermometer uses a K type thermocouple. A thermocouple measures temperature by producing an electrical potential difference between two dissimilar metals. This potential difference is then related to a temperature. A K type thermocouple is made of a chromel metal and an alumel metal. The chromel metal is 90% nickel and 10% chromium. The alumel metal is 95% nickel, 2% manganese, 2% aluminum and 1% silicon [Concept Alloys Inc., 2009]. This is the most common type of thermocouple used in thermometers because of its relatively small expense. According to the Omega Digital Thermometer operations manual, the device has an uncertainty of ± (0.5% of reading + 0.5 K) and a resolution of 0.1 K for a temperature range of 233 K to 473 K. The device also has an uncertainty of ± (1.0% of reading + 1 K) and a resolution of 1 K for a temperature range of 153 K to 2272 K [Omega, 2008].

A Yokogawa Temperature Input Meter was used to monitor the temperatures of the feed water and the boiler exhaust. The meters provide a digital output of temperature in degrees Fahrenheit and are reported to the tenths place. The meters that the power plant uses to record data have been discontinued by Yokogawa. For this reason, the manual for a similar replacement model was used to reference for uncertainties. A thermocouple is used to measure temperatures. This process is similar to that of the Omega Digital Thermometer. The Yokogawa meters are

able to interface several different types of thermocouples. Since it is not certain which thermocouples the power plant is using, the uncertainties associated with the measurements were taken to be those of the thermocouple with the greatest uncertainty as noted in the operator's manual. The meter has a resolution of 0.1 K. The thermocouple used has a temperature range of 225 K to 1250 K. According to the Yokogawa operator's manual, the uncertainty for this temperature range is $\pm$ 2 K [Yokogawa, 2011].

The temperature of the condensate tank is measured with an Ashcroft Bimetal Thermometer. The thermometer uses a bimetallic coil to display an analog reading of the temperature. The range of temperature for this thermometer is from 0 degrees Fahrenheit to 250 degrees Fahrenheit. According to the operator's manual for this device, the uncertainty over its entire temperature span is $\pm$ 1% of the reading [Aschcroft, 2011]. The device has a minor graduation of 1 degree Fahrenheit. This implies that the uncertainty in the analog reading of the scale is $\pm$ 0.5 degrees Fahrenheit. Therefore the uncertainty in temperature values recorded using this thermometer is the sum of 0.5 degrees Fahrenheit and 1.0% of the recorded value.

The temperatures for different parts in the heat recovery system were recorded with three Trerice Dial Thermometers. These dial thermometers use bimetallic coils to actuate the needle of the dial, similar to the thermometer of the condensate tank. All three dial thermometers have a recording range of 30 degrees Fahrenheit to 300 degrees Fahrenheit. According to the owner's manual for this thermometer, the uncertainty for this range of temperatures is $\pm$ 1 scale division. The minor graduation of these dials is 1 degree. Therefore the dial thermometers have an uncertainty of $\pm$ 1 degree Fahrenheit.

The rate of energy production is measured using a Crompton Switchboard Integra, Model 1540. The Crompton Switchboard Integra device is a multifunctional metering device that is able

to record multiple electrical signals simultaneously. The only measurement of this device which was considered for this experiment was the rate of energy production. According to the owner's manual, this device has an uncertainty of $\pm$ 0.9% of the reading for measurements of energy rate production. Table 8 summarizes the preceding discussion of uncertainties.

Table 8: Physical value measured at the SJU power plant, the instrument which measured it and the respective uncertainty calculation for each measured value:

Physical Value	Instrument Used	Uncertainty
CH_4 Concentration	Gas Chromatography – Flame Ionization	$\pm$ 2% of recorded value
CO Concentration	Gas Chromatography – Flame Ionization	$\pm$ 2% of recorded value
CO_2 Concentration	Gas Chromatography – Thermal Conductivity	$\pm$ 2% of recorded value
Steam Flow Rate to Turbine	Orifice-Plate Flow Meter	$\pm$ 3% of recorded value
Gas Flow Rate	Orifice-Plate Flow Meter	$\pm$ 3% of recorded value
Steam Flow Rate to Campus	Prowirl 73 Meter	$\pm$ 2.3% of recorded value
HP Steam Pressure	Ashcroft Duragauge – 0 psig to 300 psig	$\pm$ (1.0 psig + 0.5% of recorded value)
Feed Water Pressure	Ashcroft Duragauge – 0 psig to 300 psig	$\pm$ (1.0 psig + 0.5% of recorded value)
LP Steam Pressure	Ashcroft Duragauge – 0 psig to 15 psig	$\pm$ (0.05 psig + 0.5% of recorded value)
DA Tank Pressure	Ashcroft Duragauge – 0 psig to 15 psig	$\pm$ (0.05 psig + 0.5% of recorded value)
Surface Temperature of Steam Pipes	Fluke 62 Mini IR Thermometer	1. 283.15 K to 303.15 K range: ($\pm$ 1 K) 2. Outside 283.15 K to 303.15 K range: ($\pm$ 1.5 K) or ($\pm$ 1.5% of value) [report greatest]
DA Tank Temperature	Alcohol Thermometer	$\pm$ 1˚F
Ambient Air Temperature	Omega Digital Thermometer (HH-25KC) Type K thermocouple	233 K to 473 K ($\pm$ (0.5% of value + 0.5 K)) 153 K to 2272 K ($\pm$ (1.0% of value + 1 K))
Feed Water Temperature	Yokogawa Temperature Input Meter - Thermocouple	$\pm$ 2 K
Exhaust Gas Temperature	Yokogawa Temperature Input Meter - Thermocouple	$\pm$ 2 K
Temperature Condensate Tank	Ashcroft Bimetal Thermometer	$\pm$ (0.5˚F + 1% of recorded value)
Temperature of Make-up Water	Trerice dial thermometer from 30-300 F	$\pm$ 1˚F
Rate of Energy Production	Crompton Switchboard Integra-Model 1540	$\pm$ 0.9% of recorded value

APPENDIX B: List of Notation

A	Surface Area (m^2)
AB	At Boiler
AT	At Turbine
BA	Feed Water after Economizer B but before Economizer A
BD	Blow-Down Water
c_P	Specific Heat Capacity – Constant Pressure (J/K*kg)
CW	Condensate Water
e	Efficiency (unitless)
FW	Feed Water
H	Enthalpy (J)
HP	High Pressure
k	Thermal Conductivity (W/m*K)
L	Thickness (m)
LP	Low Pressure
L_v	Latent Heat of Vaporization (J/kg)
m	Mass (kg)
MW	Make-Up Water
n	Number of Moles
NG	Natural Gas
P	Pressure (Pa)
R	Universal Gas Constant = 8.315 J/(mol*K)
STP	Standard Temperature & Pressure
T	Temperature (K)
t	Time (s)
V	Volume (m^3)
W	Work (J)
$\Delta_f H$	Enthalpy of Formation
ε	Emissivity (unitless)
σ	Stefan-Boltzmann Constant = 5.6704 * 10^(-8) W/(m^2*K^4)
δ	Difference in Value

APPENDIX C: Determination of Internal Steam Temperature

The SJU power plant does not have thermometers to record steam temperature as it

leaves the boiler, or as it enters the turbine. Instead, the power plant uses handheld thermometers

that use properties of emissivity and radiation to determine the surface temperature of wherever a

reference laser is pointed towards. The SJU power plant uses a device called a Fluke 62 Mini IR

Thermometer which is described in Appendix B. Since this value is a surface temperature of the

pipe and not the actual temperature of the steam, thermodynamic properties of radiation and

conduction where applied to determine the internal temperature of the steam. Heat from the steam conducts through the walls of the transport pipe and once the heat reaches the outside surface of the pipe, it radiates throughout the room as depicted in Figure 5. Therefore the rate of heat transfer by radiation must be equal to the rate of heat transfer by conduction. This is more simply stated as, any heat leaving the pipe through conduction, must enter the space surrounding the pipe:

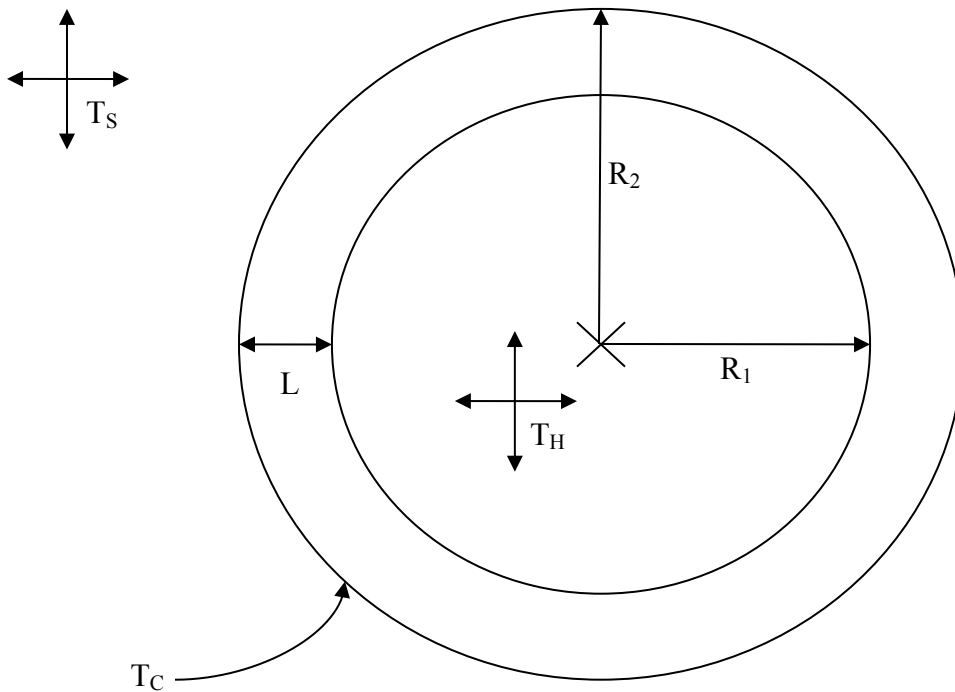$$\frac{dH_{Conduction}}{dt} = \frac{dH_{Radiation}}{dt} \tag{139}$$

Figure 5: Schematic of steam transport pipe. SJU Power Plant uses Schedule 40 steel piping for transporting steam.

The equations for conduction and radiation heat transfer are known to be the following [Young & Freedman, 2008]:

$$\frac{dH_{Conduction}}{dt} = kA\frac{T_H - T_C}{L} \tag{140}$$

$$\frac{dH_{Radiation}}{dt} = A\varepsilon\sigma(T_C^4 - T_S^4) \tag{141}$$

Following the assumption that all the heat which conducts through the pipe enters the room:

$$A\varepsilon\sigma(T_C^4 - T_S^4) = kA\frac{T_H - T_C}{L} \tag{142}$$

Solving this expression for T_H allows for the internal temperature of the steam to be determined using recorded data values of T_C and T_S:

$$T_H = T_C + \frac{(R_2 - R_1)\varepsilon\sigma}{k}(T_C^4 - T_S^4) \tag{143}$$

The emissivity of steel piping varies significantly due to different surface coloring and texture. For this reason, an average value of reported values for the emissivity of steel was used and the reported uncertainty is the standard deviation of these values [The Engineering Toolbox, 2013] and [Omega, 2013]. The thermal conductivity of steel is less ambiguous and is reported below [Young & Freedman, 2008]:

$$\varepsilon = 0.820 \pm 0.048 \tag{144}$$

$$k_{Steel} = 50.2 \pm 0.5 \frac{W}{m \cdot K} \tag{145}$$

The SJU power plant uses schedule 40 piping for transport of steam [Vogel, 2013]. Schedule 40 pipe has an internal radius of R1 = 3.99 inches = 10.13 $\pm$ 0.10 cm and external radius of R2 = 4.32 inches = 10.96 $\pm$ 0.11 cm [The Engineering Toolbox, 2013]. The difference between these two radii gives the thickness of the piping. With the information listed, by recording the room temperature of ambient air and by recording the surface temperature of the piping with the infrared thermometer, the internal temperature of the steam pipe was determined.

APPENDIX D: Derivation of Atmospheric Pressure at SJU Power Plant[7]

To use the steam tables to obtain values for our system, we first need to decide on an atmospheric pressure to relate gauge pressure to absolute pressure. Gauge pressure reads pressure relative to whatever the atmospheric pressure at that gauge is:

$$p_{gauge} = p_{abs} - p_{atm} \tag{146}$$

Atmospheric pressure decreases as elevation increases; at sea level, atmospheric pressire is 14.696 psi. Average atmospheric pressure at any elevation can be calculated by using a series of formulas.[8] First, geometric elevation Z in meters (m) must be converted to geopotential elevation H in geopotential meters (m'):

$$H = \Gamma \left(\frac{r_0 \cdot Z}{r_0 + Z} \right) \tag{147}$$

where $\Gamma = g_0/g_0' = 1 \, m'/m$, and $r_0 = 6\,356\,766 \, m$. Then, the atmospheric pressure p is found from geopotential elevation H:

$$p = p_b \left[\frac{T_{M,b}}{T_{M,b} + L_{M,b} \cdot (H - H_b)} \right]^{\left[\frac{g_0' \cdot M_0}{R^* \cdot L_{M,b}} \right]} \tag{148}$$

where

$$R^* = 8.314\,32 \times 10^3 \, \frac{N \, m}{kmol \, K} \tag{149}$$

$$g_0' = 9.806\,65 \, \frac{m}{s^2 \, m'} \tag{150}$$

$$H_b = 0 \, km' \, (for \, H < 11 \, km') \tag{151}$$

---

[7] *Please note that the derivation included in this appendix is not that of the author of this report. The derivation is the original unpublished work of Nicholas Moe. Verbal permission was given to the author by Mr. Moe to publish his derivation in this report. The work of Appendix B belongs entirely to Mr. Moe, including any foot notes.*

[8] National Oceanic and Atmospheric Administration, National Aeronautics and Space Administration, and United States Air Force, *U.S. Standard Atmosphere, 1976* (Washington, D.C.: October 1976), 8-12, http://ntrs.nasa.gov/archive/nasa/casi.ntrs.nasa.gov/19770009539_1977009539.pdf.

$$L_{M,b} = -0.0065 \frac{K}{m'} \tag{152}$$

$$p_b = p_0 \; for \; b = 0; \; p_0 = 101 \; 325.0 \frac{N}{m^2} \tag{153}$$

$$T_{M,b} = T_{M,0} \; for \; b = 0; \; T_{M,0} = T_0 = 288.15 \; K \tag{154}$$

Table 9: Average atmospheric pressure at sea level and for a range of elevations on the **Saint John's campus.**

Elevation ft, MSL	Pressure psi	Pressure kPa
0	14.696	101.325
1160	14.090	97.149
1165	14.088	97.132
1170	14.085	97.114
1175	14.083	97.096
1180	14.080	97.078
1185	14.077	97.061
1190	14.075	97.043
1195	14.072	97.025
1200	14.070	97.008
1205	14.067	96.990
1210	14.065	96.972

A listing of atmospheric pressures at elevations on the Saint John's campus is given in Table 9.

The main floor of the Power House is at a geometric elevation of approximately 1185 ft. Since some meters are above the main floor and some are below, this elevation serves as an average. The atmospheric pressured used to convert gauge pressure to absolute pressure for the metering system shall be 97.061 kPa (14.077 psi).

Here is a derivation of the 0.3315 factor used to convert the volumetric flow rate of natural gas to a molar flow rate. The natural gas is measured in kilo-standard cubic feet per hour. The standard cubic foot (scf) used in this measurement is at a temperature of $T = 60 \,°F$ and a pressure of $P = 14.73 \, psi$ [Moe, 2012]. Converting these values to SI units yields $T = 289 \, K$ and $P = 101.6 \, kPa$. The ideal gas law allowed for the determination of a molar flow rate from a volumetric flow rate:

$$PV = nRT \tag{155}$$

$$\frac{dn}{dt} = \frac{P}{RT}\frac{dV}{dt} \tag{156}$$

Finally the volumetric flow rate was converted to SI units. Below is the conversion:

$$[kscfh] = 1{,}000 \frac{ft^3}{hour} \frac{1 \, hour}{60 \, minutes} \frac{1 \, minute}{60 \, seconds} \frac{1 \, m^3}{3.28084^3 ft^3} = 0.007866 \frac{m^3}{second} \tag{157}$$

This value was then multiplied by the flow rate in units of kscfh to calculate the volumetric flow rate in SI units:

$$\frac{dV}{dt}\left[\frac{m^3}{second}\right] = \frac{0.007866 \dfrac{m^3}{second}}{1 \, kscfh} * \frac{dV}{dt}[kscfh] \tag{158}$$

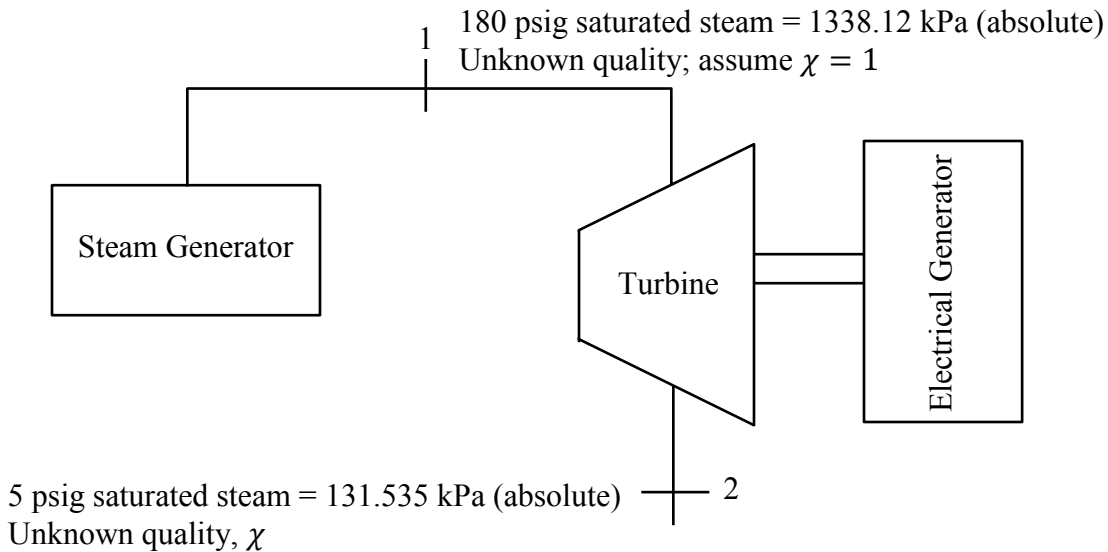Combining this value with the ideal gas law, the conversion factor reported in the Methods and Theory section was found:

$$\frac{dn}{dt} = \left[\frac{(101.6 \times 10^3 \, \text{Pa})}{\left(8.31 \frac{J}{mole \cdot K}\right)(289 \, K)}\right]\left[0.007866 \frac{m^3}{second}\right]\left[\frac{dV}{dt}[kscfh]\right] \tag{159}$$

$$= 0.33315 \left[\frac{moles}{second \cdot kscfh}\right] * \frac{dV}{dt}[kscfh] \tag{160}$$

<u>APPENDIX F:</u> Steam Quality Derivation[9]

<u>Analysis of Saint John's Turbine # 3</u>

1 — 180 psig saturated steam = 1338.12 kPa (absolute)
Unknown quality; assume $\chi = 1$

2

5 psig saturated steam = 131.535 kPa (absolute)
Unknown quality, χ

Atmospheric pressure: 97.061 kPa (14.077 psi). At 5:38 PM on 21 Dec 2012, turbine 3 was generating 589.8 kW from 9,401.4 kg/h going through the turbine.

Let's assume that the work the turbine is doing is equal to that of the electrical generator, i.e. assume that the electrical generator is 100 % efficient. In actuality, the work of the turbine is greater than the work output by the generator.

We don't know the quality of the incoming steam, but since it goes through a steam separator before the steam goes through the turbine, assume that $\chi_1 = 1$.

State	Temp (°C)	Pressure	Entropy	Enthalpy
1	192.946	1338.12 kPa (absolute)	6.4836 kJ/kg K	0.774290 kWh/kg
		13.3812 bar	1.800972×10^{-3} kWh/kg K	2787.444 kJ/kg
2	107.4533	131.535 kPa (absolute)	TBD	TBD
		1.31535 bar		

---

[9] *Please note that the derivation included in this appendix is not that of the author of this report. The derivation is the original unpublished work of Nicholas Moe. Verbal permission was given to the author by Mr. Moe to publish his derivation in this report. The work of Appendix D belongs entirely to Mr. Moe, including any foot notes*

$$\eta_{turb} = \frac{h_1 - h_2}{h_1 - h_{2s}} \tag{161}$$

$$h_2 = h_1 - \eta_{turb}(h_1 - h_{2s}) \tag{162}$$

Where η_{turb} is the isentropic efficiency, h_1 is the actual specific enthalpy of state one, h_2 is the actual specific enthalpy of state two and h_{2s} is the specific enthalpy of state two for a perfectly isentropic turbine [Young & Freedman, 2008]. If the turbine were ideal and hence isentropic, the entropy would not change as the steam goes through the turbine. The conditions under these assumptions would be:

$$h_{2s} = 2389.0154 \; kJ/kg \tag{163}$$

$$s_{2s} = 6.4835 \; kJ/kg \tag{164}$$

The turbine's work, assuming that all the energy in the HP steam is converted into electrical work, is:

$$w_t = h_1 - h_{2g} \tag{165}$$

Where w_t is the work of the turbine. h_1 and h_{2g} are the specific enthalpies of the steam in states one and two respectively, assuming all the energy in the HP steam is converted to electrical work. We know w_t and h_1, so:

$$h_{2g} = h_1 - w_t \tag{166}$$

We need to convert the turbine work before we can use it:

$$w_t = \frac{589.8 \; kJ}{s} \frac{3600 \; s}{1 \; h} \frac{1 \; h}{9401.4 \; kg} = 225.847 \frac{kJ}{kg} \tag{167}$$

$$h_{2g} = h_1 - w_t = 2787.444 \; kJ/kg - 225.847 \; kJ/kg = 2561.597 \; kJ/kg \tag{168}$$

$$\eta_{turb} = \frac{h_1 - h_2}{h_1 - h_{2s}} = \frac{2787.444 \; kJ/kg - 2561.597 \; kJ/kg}{2787.444 \; kJ/kg - 2389.0154 \; kJ/kg} = 0.567 \tag{169}$$

The quality of steam is defined as [Young & Freedman, 2008]:

$$\chi = \frac{h_2 - h_\ell}{h_v - h_\ell} \tag{170}$$

$$h_2 = \chi h_v + h_\ell(1 - \chi) \tag{171}$$

$$h_2 = h_1 - \eta_{turb}(h_1 - h_{2s}) \tag{172}$$

$$\chi = \frac{h_1 - \eta_{turb}(h_1 - h_{2s}) - h_\ell}{h_v - h_\ell} \tag{173}$$

Where h_ℓ is the specific enthalpy of liquid water and h_v is the specific enthalpy of water vapor (steam). For saturated steam at 5 psig:

$$h_\ell = 450.5859 \; kJ/kg \tag{174}$$

$$h_v = 2687.1777 \; kJ/kg \tag{175}$$

$$h_v - h_\ell = 2236.5918 \, kJ/kg \tag{176}$$

It must be true that the actual specific enthalpy of state two (h_2) be greater than the specific enthalpy of state two for a perfectly isentropic turbine (h_{2s}). It must also be true that the actual specific enthalpy of state two (h_2) be less than the specific enthalpy of state two assuming that all of the energy provided to generator by the turbine is converted to electrical work (h_{2g}):

$$h_{2s} < h_2 < h_{2g} \tag{177}$$

Using these two conditions, we may find a bound on the quality of the low pressure steam leaving the turbine at state two:

$$h_2 > h_{2s} \tag{178}$$

$$\chi h_v + h_\ell(1 - \chi) > h_{2s} \tag{179}$$

$$\chi(h_v - h_\ell) > h_{2s} - h_\ell \tag{180}$$

$$\chi > \frac{h_{2s} - h_\ell}{h_v - h_\ell} \tag{181}$$

$$h_2 < h_{2g} \tag{182}$$

$$\chi h_v + h_\ell (1 - \chi) < h_{2g} \tag{183}$$

$$\chi (h_v - h_\ell) < h_{2g} - h_\ell \tag{184}$$

$$\chi < \frac{h_{2g} - h_\ell}{h_v - h_\ell} \tag{185}$$

$$\frac{h_{2s} - h_\ell}{h_v - h_\ell} < \chi < \frac{h_{2g} - h_\ell}{h_v - h_\ell} \tag{186}$$

Since all of the values listed above have been determined, we are able to find a range of steam quality for state two:

$$\frac{2389.0154 \; kJ/kg - 450.5859 \; kJ/kg}{2236.5918 \; kJ/kg} < \chi$$

$$< \frac{2561.597 \; kJ/kg - 450.5859 \; kJ/kg}{2236.5918 \; kJ/kg} \tag{187}$$

$$0.86669 < \chi < 0.94385 \tag{188}$$

The middle of this range shall be the reported value for the quality of the low pressure steam leaving the steam turbine. Half of the difference between the maximum and minimum steam quality values determined the uncertainty:

$$\chi = 0.905 \pm 0.039 \tag{189}$$

APPENDIX G: Low Pressure Steam Pipe Lengths

Table 10: Summary of campus buildings that receive heat by steam produced at the SJU power plant. All reported values have units of meters.

Campus Building	Short Distance	Long Distance	Average Distance	Uncertainty
Benet Hall	194	220	207	13
Bernard Hall	195	235	215	20
Boniface Hall	298	334	316	18
Emmaus Hall	130	179	155	25
Frank House	82	112	97	15
Joseph Hall	56	81	69	13
Mary Hall	243	307	275	32
Maur House	344	359	352	8
Patrick Hall	257	310	284	27
Placid House	343	360	352	9
Thomas Hall	106	171	139	33
Virgil Michel House	303	324	314	11
Greg House	94	110	102	8
Quadrangle	154	232	193	39
Great Hall	211	238	225	14
Abbey Church	292	329	311	19
Breuer Wing	247	324	286	39
Peter Engel	436	509	473	37
New Science	507	554	531	24
Alcuin Library	356	421	389	33
Hill Museum	343	360	352	9
Warner Palestra	482	570	526	44
Art Center	148	166	157	9
SJU Pottery Studio	81	104	93	12
Physical Plant	26	47	37	11
Fire Hall	48	68	58	10
Wimmer Hall	150	170	160	10
Saint Luke Hall	126	149	138	12
Liturgical Press	67	103	85	18
Guild Hall	106	134	120	14
Simmons Hall	167	197	182	15
Sexton Commons	234	263	249	15
Music Hall	242	277	260	18

APPENDIX H: Conversion Factors Used

Table 11: Two column table where the left column (Value 1) is equal to the right column (Value 2):

Value 1	Value 2
1 psi	6 894.75729 Pa
1 pound	4.44822162 N
3.28084 feet	1 meter
1 torr	133.3223689 Pascals
1 cubic foot	0.0283168 cubic meters
1 inch	2.54 cm
Gravitational Acceleration (g)	9.806 m/s^2
Molar Mass of Water	18.0153 g/mol
Ideal Gas Constant (R)	8.135 J/mol K

REFERENCES:

Architect of the Capitol. (2013). Capitol Power Plant Cogeneration Project (Rep. No.

    202.228.1793). Retrieved from

    http://www.aoc.gov/sites/default/files/CPP_Cogen_Fact%20sheet.pdf

Background. (2010). NaturalGas.org. Retrieved from

    http://www.naturalgas.org/overview/background.asp

Bimetal thermometer accuracy definitions (p. 1, Tech. No. 256). (2011). New York City, NY:

    Aschcroft.

Blasing, T. J. (2013, February 20). *Carbon Dioxide Information Analysis Center* (The United

    States of America, U.S. Department of Energy, Office of Science). Retrieved from

    http://cdiac.ornl.gov/pns/current_ghg.html

Calculate thermodynamic and transport properties of water and steam. (2008). Steam Tables

    Online. Retrieved from http://www.steamtablesonline.com/steam97web.aspx

DOE, Combined heat and power: a federal manager's resource guide (Final Report), US

    Department of Energy, Federal Energy Management Program, 2000.

Economical, high performance handheld thermometers (pp. 1-2, Tech.). (2008). Stamford, CT:

    Omega.

Energy and sustainability. (2013). *College of Saint Benedict and Saint John's University:*

    OSB/SJU Physical Plant. Retrieved from http://csbsju.edu/SJU-Physical-Plant/Energy-

    and-Sustainability.htm

Fluke 62 mini infrared thermometer (pp. 1-2, Tech.). (2008). Everett, WA: Fluke Corporation.

Gary, W. (January 01, 2010). Evaluating deaerator operation. *Hpac Heating, Piping,*

    Airconditioning Engineering, 82, 1.)

Google. (2013). Google maps. *Google Maps*. Retrieved from https://maps.google.com/

Informational postings (2013). Northern Natural Gas: A MidAmerican Energy Holdings

    Company. Retrieved from

    http://www.northernnaturalgas.com/infopostings/GasQuality/Pages/GasQualityById.aspx

Jones, J. B., & Hawkins, G. A. (1986). *Engineering thermodynamics* (2nd ed.). Wiley, NY.

Karmen, A., & Haut, H. (1973). Alkali Flame Ionization Detector Attachment for Conventional

    Hydrogen Flame Ionization Detectors. *Analytical Chemistry*, *45*, 822-824.

Kebbekus, B. B., Barsky, M. H., Rossi, R. T. & Jordan, J. (1965). Quantitative gas

    chromatography with thermal conductivity detectors – a fundamental approach based on

    kinetic theory. *Journal of the American Chemical Society, 88*, 2398-2403.

Kevin, S., Mazzeo, A., & Tetra Tech Em Inc. (2010). *Final Indoor Ambient Air Monitoring and*

    Assessment Plan for the Lower Darby Creek Area (pp. 1-15, Rep. No. E43-028-10-01-

    001). PA: Environmental Protection Agency.

Lide, D. R. (2007). *CRC Handbook of Chemistry and Physics 87th Edition* (p. 5-4 – 42, 6-9 & 6-

    2). Boca Raton, FL: CRC Press – Taylor & Francis Group.

Material safety data sheet. (pp. 1, Tech.). (2009). Whitmore Lake, MI: Concept Alloys, Inc.

McMurry, J.E. & Fay, R. C. (2010). Gases: their properties and behavior: gases and gas pressure.

    In *General chemistry: atoms first* (p. 306). Upper Saddle River, NJ: Pearson Prentice

    Hall.

Moe, N. (2012, October 15). [OSB/SJU Metering Re-calibration and Setup]. Unpublished raw

    data.

Moe, N. (2013). [Derivation of Low Pressure Steam Quality for Saint John's University Power

    Plant]. Unpublished raw data.

Molina, M. J., & Rowland, F. S. (1974). Stratospheric sink for chlorofluoromethanes: Chlorine atomic-atalysed destruction of ozone. *Nature Publishing Group*, 810-812.

National Oceanic and Atmospheric Administration. (2012, May 7). Air pressure. *National Weather Service - JetStream - Online School for Weather*. Retrieved from http://www.srh.noaa.gov/jetstream/atmos/pressure.htm

Omega.com. (2013). Emissitivity of common materials. *Omega*. Retrieved from http://www.omega.com/literature/transactions/volume1/emissivitya.html

Potvin, P. (1999). *New boiler at St. John's University* (pp. 1-8, Rep.). St. Paul, MN: Lundquist, Killeen, Potvin & Bender.

Power Plant. (2013). *College of Saint Benedict and Saint John's University*. Retrieved from http://csbsju.edu/SJU-Physical-Plant/Shops/Power-Plant-Original.htm

Proline prowirl 72F, 72W, 73F, 73W - vortex flow measuring system reliable flow measurement of gas, steam and liquids (pp. 1-63, Tech. No. 71128149). (2011). Switzerland: Andress+Hauser.

Saint John's University (1945, June 28). New plant plans completed. The Record: Official Newspaper of St. John's University and Organ of the Alumni, p. 1.

Schroeder, D. V. (2000). *An introduction to thermal physics* (pgs. 6, 18, 28, 134, 135 & 404). San Francisco, CA: Addison Wesley.

Simpson, I. J., Akagi, S. K., Barletta, B., Blake, N. J., Choi, Y., Diskin, G. S., Fried, A., Fuelberg, H. E., Meinardi, S., Rowland, F. S., Vay, S. A., Weinheimer, A. J., Wennberg, P. O., Wisthaler, A., Yang, M., Yokelson, R. J. & Blake, D. R. (2011). Boreal forest fire emissions in fresh Canadian smoke plumes: C1-C10, volatile organic compounds

(VOCs), CO2, CO, NO2, NO, HCN and CH3CN. *Atmospheric Chemistry and Physics, 11*, 6445-6463.

Simpson, I. J., Blake, D. R., & Rowland, F. S. (2002). Implications of the recent fluctuations in the growth rate of tropospheric methane. *Geophysical Research Letters, 29*(10), 117-120.

Simpson, I. J., Rowland, F. S., Meinardi, S., & Blake, D. R. (2006). Influence of biomass burning during recent fluctuations in the slow growth of global tropospheric methane. *Geophysical Research Letters, 33*(LL22808), 1-5.

Steam Tables. (2013). *Spirax Sarco USA*. Retrieved from http://www.spiraxsarco.com/us/resources/steam-tables.asp

Steel pipes dimensions - ANSI schedule 40. (n.d.). *The Engineering Toolbox*. Retrieved from http://www.engineeringtoolbox.com/ansi-steel-pipes-d_305.html

Steven, R. and Hall, A. (2009). Orifice plate meter wet gas flow performance. *Flow Measurement and Instrumentation, 20,* 141-151.

Stultz, S. C., & Kitto, J. B. (2005). Introduction to steam. In *Steam: Its generation and use* (41st ed., pp. Intro-1). Barberton, OH: Babcock & Wilcox.

Taylor, J. R. (1997). *An introduction to error analysis: The study of uncertainties in physical measurements*. Sausalito, CA: University Science Books.

The Engineering ToolBox. (2013). Emissivity coefficients of some common materials. *Www.EngineeringToolBox.com*. Retrieved from http://www.engineeringtoolbox.com/emissivity-coefficients-d_447.html

Type 2452 Duragauge pressure gauge with PLUS performance option (pp. 1-2, Tech. No. DU-4 2462). (2009). Stratford, CT: Ashcroft.

United States of America, Department of Energy, Energy Information Administration.

(2011). *International energy statistics*. Washington, DC: Government of the United States
of America.

University of Michigan. (2010). Cogeneration at the central power plant. Occupational Safety
and Environmental Health. Retrieved from http://www.p2000.umich.edu/energy-
conservation/ec4.htm

Vogel, T. (2013, February 12). Senior thesis discussion [Personal interview].

What is cogeneration? (2010). Intelligen Power Systems LLC – Intelligent Cogeneration.
Retrieved from http://www.intelligentpower.com/whatiscogen.htm

Young, H. D., Freedman, R. A., Ford, A. L., Sears, F. W., & Zemansky, M. W. (2008). *Sears and
Zemansky's university physics.* (12th ed.). San Francisco [Calif.: Pearson Addison-
Wesley.

YPP7000 temperature input meter instruction manual (pp. 1-88, Tech. No. LIM7000YK_A).
(2011). Newnan, GA: Yokogawa Corporation of America.